Soil drying induces widespread productivity loss but unequal climate vulnerability among ecotypes of a foundational Arctic sedge

Jonathan Gewirtzman[1]*, Ned Fetcher[2]

[1]School of the Environment, Yale University, New Haven, CT, USA

[2]Institute for Environmental Science and Sustainability, Wilkes University, Wilkes-Barre, PA, USA

*** Correspondence:**

Jonathan Gewirtzman

jonathan.gewirtzman@yale.edu

Abstract

1. As temperatures increase in the Arctic, hydrological change may lead to local soil drying through altered snowpack, evapotranspiration, and drainage due to permafrost thaw. These changes threaten to alter soil moisture regimes that control plant productivity and ecosystem carbon cycling.
2. *Eriophorum vaginatum*, a foundational sedge that accounts for up to 30% of carbon uptake in moist tundra ecosystems, exhibits substantial local adaptation across its range, yet its capacity to maintain productivity under changing soil moisture conditions remains unknown.
3. We conducted a common garden experiment using tussocks from three populations along a latitudinal gradient in northern Alaska, subjecting them to treatments simulating both surface soil drying and deeper drainage from permafrost thaw.
4. Through measurements of plant water status, photosynthetic capacity, and seasonal growth patterns, we found that soil drying substantially reduced productivity across all populations through both decreased photosynthesis and reduced leaf area. Plants responded to moisture stress primarily by reducing canopy size and accelerating senescence rather than altering leaf-level physiology, with southern populations showing greater vulnerability to drought stress.
5. Our findings highlight regional differences in drought susceptibility and suggest that shifts in soil moisture could influence Arctic plant productivity and carbon cycling under future climate.

1. Introduction

Arctic warming is fundamentally altering ecosystem water balance through changes in precipitation patterns, permafrost thaw, and increasing evaporative demand. Permafrost, which acts as a barrier to vertical water flow, creates perched water tables and saturated soils in the active layer. As permafrost thaws and the active layer deepens, these hydrological controls weaken, potentially leading to soil drying in some areas and localized saturation in others due to ground subsidence and thermokarst formation (Jorgenson et al., 2001; Lawrence et al., 2015). Model intercomparisons predict surface soil drying across the permafrost region despite increased precipitation and evapotranspiration, due to deeper moisture infiltration as thaw progresses, though there is significant uncertainty in the magnitude and spatial patterns of these projections (Andresen et al., 2020). These shifts in soil hydrology may emerge as key drivers of Arctic carbon cycling through their effects on both microbial decomposition and plant productivity.

Understanding the relationship between soil moisture dynamics and ecosystem carbon fluxes remains a critical research frontier in Arctic ecology. While some studies show that drying can amplify warming effects on soil respiration (Natali et al., 2015), vegetation responses appear more complex. Water table manipulations have produced contradictory results, with flooding increasing productivity in lowland tundra (Chivers et al., 2009), whereas drying has minimal effects in upland systems (Natali et al., 2015). Remote sensing reveals that increased precipitation can decrease productivity in some regions (Lara et al., 2018), while climate extremes generally reduce plant growth (Phoenix & Bjerke, 2016). The variable nature of these responses suggests that understanding species-specific adaptations to moisture stress is crucial for predicting ecosystem-level changes.

Plant responses to changing water availability in the Arctic will depend on both soil moisture and atmospheric water demand. Water availability and drainage depth have been shown to limit Arctic plant productivity, with topographic variation playing a key role in regulating xylem pressure potential, sap flow, and water-use efficiency (Black et al., 2021; Oberbauer & Miller, 1979). While soil moisture changes may be spatially heterogeneous due to local topography and permafrost conditions, increasing vapor pressure deficit (VPD) is expected to be widespread as temperatures rise (Grossiord et al., 2020). High VPD can trigger drought-like responses in plants even when soil moisture is adequate (Sulman et al., 2016), potentially

amplifying the effects of soil drying. These individual or combined stressors may be particularly important for tundra species that historically evolved under cool, moist conditions. Understanding how foundation species respond to both soil and atmospheric water stress is therefore critical for predicting Arctic ecosystem responses to climate change.

Changes in Arctic hydrological dynamics are expected to influence vegetation composition and productivity. Foundation species, which exert a disproportionate influence on ecosystem structure and function, are especially important in this context because their responses to water limitation can cascade through the ecosystem, affecting carbon cycling at multiple scales. One such foundation species in Arctic tundra ecosystems is *Eriophorum vaginatum* L., a tussock-forming sedge that shapes microclimatic variation and supports plant communities through its growth habit (Chapin et al., 1979; Shaver et al., 2001). As a dominant species accounting for up to 30% of annual carbon uptake in some tundra ecosystems, *E. vaginatum* plays a crucial role in Arctic ecosystem structure and productivity (Chapin & Shaver 1985; Shaver et al., 2001). The ability of *E. vaginatum* to exploit subsurface water flow and the dissolved nutrients it carries may partially explain its dominance in these systems (Chapin et al., 1988) and suggests that changes in soil hydrology could disproportionately affect its productivity.

The species exhibits significant intraspecific variation across its range through locally adapted populations, or ecotypes - genetically distinct populations adapted to their local environments. These ecotypes differ in traits including phenology, growth rate, and resource allocation (Bennington et al., 2012; Parker et al., 2017), documented through both latitudinal gradient observations and reciprocal transplant experiments (Fetcher & Shaver, 1990; Schedlbauer et al., 2018). However, as a long-lived species (Mark et al., 1985), *E. vaginatum* may struggle to adapt quickly enough to rapid environmental change, a phenomenon known as adaptational lag (McGraw et al., 2015).

Evidence suggests that water relations vary among populations, with northern populations showing higher stomatal density that may reduce water use efficiency (Peterson et al., 2012). However, the functional significance of this variation for drought tolerance remains unknown. Understanding how locally adapted populations respond to moisture stress is crucial, as ongoing changes in Arctic hydrology may create mismatches between historical adaptations and current conditions, with consequences for tundra ecosystem function.

To better understand how this foundational sedge responds to changing moisture conditions, we conducted a common garden experiment with three ecotypes from a latitudinal gradient in northern Alaska. We asked: (1) How do changes in soil moisture availability affect *E. vaginatum* productivity and water relations? (2) Does deeper soil drainage elicit different responses than surface drying alone? (3) Are drought responses consistent across ecotypes despite local adaptation to different moisture regimes? By measuring plant water status, photosynthetic capacity, and seasonal growth patterns, we aimed to assess how ecotypic variation influences drought tolerance and to elucidate the implications of these responses for future Arctic ecosystem dynamics.

2. Methods

2.1.1. Study sites

We collected *Eriophorum vaginatum* tussocks from three sites along a latitudinal gradient in northern Alaska (Figure 1): Sagwon (SG; 69.4245°N, 148.6946°W, elev. 300 m), Toolik Lake (TL; 68.6269°N, 149.5975°W, elev. 760 m), and Coldfoot (CF; 67.2528°N, 150.1847°W, elev. 331 m). These sites have been the focus of long-term ecological research on *E. vaginatum* adaptation and response to environmental change (Bennington et al., 2012; Chandler et al., 2015; Fetcher & Shaver, 1990; Parker et al., 2017; Shaver et al., 1986; Souther et al., 2014). The sites represent distinct ecological and glacial histories: Sagwon at the northern edge of moist acidic tundra (potentially unglaciated during the Pleistocene), Toolik Lake in moist acidic tundra (glaciated during Late Wisconsinan, ~20,000 years BP), and Coldfoot at the taiga ecotone (glaciated during Early but not Late Wisconsinan). Environment and site histories have resulted in *E. vaginatum* populations that are genetically structured along a latitudinal gradient, with a significant barrier to gene flow at the treeline (Stunz et al., 2022).

2.1.2. Common garden design

We established a common garden experiment at Toolik Field Station in June 2017. Using established protocols (McGraw et al., 2015; Parker et al., 2017), we harvested tussocks between June 12-23, before spring green-up and root initiation (Ma, Parker, Fetcher, et al., 2022; Ma, Parker, Unger, et al., 2022). Eighteen tussocks from each population were randomly assigned to three drying treatments for a total of 54 experimental units.

2.1.3. Drying treatments

Treatments were designed to simulate three soil moisture regimes:

- Control treatment ("Wet"): Tussocks planted in 2-gallon nursery pots with peat soil, with a closed bottom to prevent drainage, maintained at saturation through natural rainfall and supplemental watering.
- Surface drying treatment ("Dry"): The pot setup identical to the Wet treatment but subjected to alternating two-week periods of rainfall exclusion using transparent tarps.
- Deep drainage and surface drying treatment ("Deep"): Tussocks planted in stacked pots with removed bottoms to create a soil column twice the depth of the Wet and Dry treatments, simulating a deepened active layer allowing deeper drainage, and also subjected to the same rainfall exclusion as the Dry treatment.

All pots were initially watered to saturation to ensure establishment. During rainfall exclusion periods, transparent tarps supported by rebar and PVC frames covered both the Dry and Deep treatment pots. Frame sides remained open to maintain airflow. Temperature and photosynthetically active radiation (PAR) were monitored inside and outside rainfall exclusion tarps, with PAR reduced by approximately 40% under tarps but no detectable temperature differences.

Soil moisture to 12cm depth was monitored weekly using a HydroSense II probe (Campbell Scientific). To convert probe readings of relative dielectric permittivity (PER) to gravimetric water content (GWC), we developed a calibration curve using five reference pots filled with peat soil. These pots were saturated with water, weighed, and monitored during drying until reaching constant mass at 105°C. A polynomial regression relating GWC to PER ($r^2 = 0.98$; Supplemental Figure S1) was used to convert field measurements to GWC.

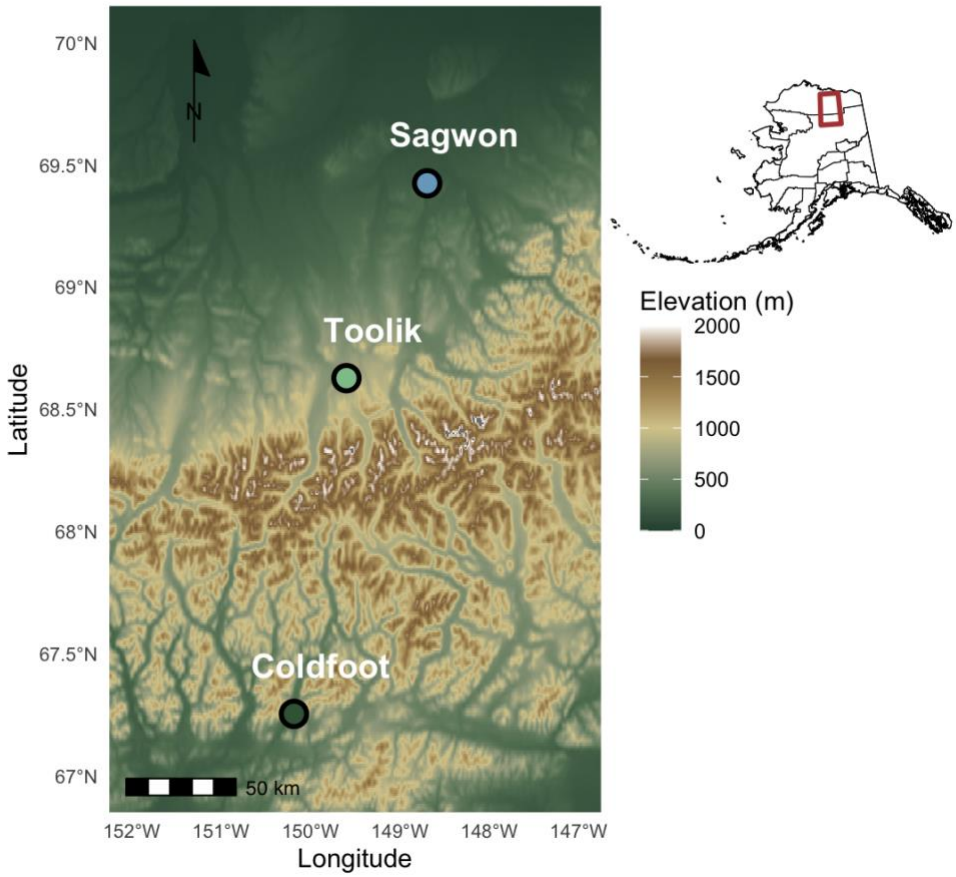

Figure 1. Map of three sites in northern Alaska, USA where Eriophorum vaginatum tussocks were collected. Background shading represents elevation (meters above sea level) derived from a composite of USGS National Elevation Dataset and Alaska IFSAR data accessed through AWS Terrain Tiles. Inset shows the location of the study area (red box) within Alaska.

2.2. Response Measurements

2.2.1. Plant Structure and Phenology

Eriophorum vaginatum is a perennial tussock-forming sedge that grows through the production of tillers, each consisting of a cluster of leaves that emerge, elongate, and senesce in sequence. We monitored tillers to capture leaf dynamics and seasonal growth patterns critical for understanding plant productivity in tundra ecosystems. We randomly selected one tiller per tussock and marked it at the base with a zip tie to track leaf development while excluding previously senesced leaves. We measured total leaf length and green leaf length weekly,

recording each individual leaf on the tiller to the nearest 5 mm to capture changes in growth and senescence throughout the growing season.

We measured normalized difference vegetation index (NDVI) using a GreenSeeker handheld crop sensor (Trimble Inc.) positioned at the minimum height required for instrument operation. We used previously established NDVI-based allometric relationships to calculate whole-tussock (canopy) leaf area index (r^2=0.88; Supplemental Figure S2) and biomass (Berner et al., 2018; Ma, Parker, Fetcher, et al., 2022).

2.2.2. Leaf-Level Physiology

We measured leaf water potential using a pressure chamber (PMS Instruments Model 600) on randomly selected tussocks from each experimental block. We cut individual leaves at the stem base and immediately measured them, continuing chamber pressurization until water appeared at the cut surface.

We measured maximum photosynthetic rate (A_{max}) using a portable photosynthesis system (LiCor LI-6400XT) on approximately five green leaves per measurement, arranged width-wise across the chamber. We conducted measurements on randomly selected tussocks on three dates (July 26, July 31, and August 8) before tiller senescence. We maintained conditions at 400ppm CO_2, 1500 μmol m^{-2} s^{-1} PAR, and ~1 kPa VPD. We calculated leaf area from measured leaf width × number of leaves × enclosed length (3 cm).

We measured CO_2 response curves on randomly selected tussocks from each block on August 2-3. We fit individual A/Ci curves using the plantecophys R package (Duursma, 2015; Farquhar et al., 1980) to estimate maximum electron transport rate (J_{max}) and maximum carboxylation rate (V_{cmax}).

2.2.3. Chemical Analysis

We estimated intrinsic water use efficiency using carbon isotope ratios ($\delta^{13}C$) (Farquhar et al., 1989). We harvested five leaves from each of three randomly selected tussocks per block at season end, dried them at 60°C for three days, ground them to powder using liquid nitrogen, and analyzed their $\delta^{13}C$ content via isotope ratio mass spectrometry at the Boston University Stable Isotope Lab.

2.3. Replication Statement

This experiment was structured as a two-way factorial design, with population (Sagwon, Toolik, and Coldfoot) and watering treatment as factors . Within each block, 18 tussocks were randomly assigned to one of three watering treatments (Wet, Dry, Deep), ensuring each treatment was applied to an equal number of individuals from each population. Measurements were conducted at multiple scales—whole tussock responses, single marked tillers per tussock for phenological tracking, and targeted subsets of plants for specific physiological traits such as photosynthetic rates and water potential.

Scale of Inference	**Scale at which the factor of interest is applied**	**Number of Replicates at the Appropriate Scale**
Ecotypic variation in *Eriophorum vaginatum* responses to drying treatments	Watering treatment applied at the level of individual tussocks	18 tussocks per treatment (54 total)
Population-level responses across a latitudinal gradient	Population as a factor applied to source locations (Sagwon, Toolik, Coldfoot)	3 populations
Individual plant-level physiological and phenological measurements	Measured on a single tiller per tussock, with different subsets used for different response variables	6 leaves/tillers per treatment per population (varied by metric)

2.4. Statistical Analysis

We used linear mixed-effects models (LME) and analysis of variance (ANOVA) to evaluate treatment and population effects across our response variables. We conducted all analyses in R (R Core Team, 2024).

We analyzed soil moisture (GWC) using an LME model with Treatment and Population as fixed effects and Tussock ID as a random effect to account for repeated measurements. We tested differences between treatments using Tukey's HSD pairwise comparisons.

For leaf-level phenology metrics (total green leaf length, average green leaf length, percent green), we fit LME models incorporating Treatment, Population, and Day of Year (DOY) as

fixed effects, with Tussock ID as a random effect. We included Treatment × DOY interaction terms to assess differences in phenological trajectories.

To analyze leaf area index (LAI), we fit a quadratic regression model to capture seasonal trajectories, with Treatment and Population as fixed effects. We calculated area under the curve (AUC) for LAI using numerical integration (trapezoidal rule) via the pracma package (Borchers, 2023) and analyzed it using a separate LME model to assess cumulative leaf area production.

We used random forest models to assess the relative importance of Treatment, Population, and Day of Year (DOY) in predicting our response variables. We trained separate random forest models for each phenological metric (total green leaf length, percent green, average green leaf length) and for LAI. For each model, we calculated variable importance using the percent increase in mean squared error (%IncMSE) when each predictor was randomly permuted. Higher %IncMSE values indicate greater importance of that variable in predicting the response. We implemented random forest models using the randomForest package (Liaw & Wiener, 2002).

We analyzed leaf water potential and photosynthetic rate (A_{max}) using two-way ANOVAs to assess Treatment, Population, and interaction effects. For A/C_i curve parameters, we fit LME models for V_{cmax} and J_{max} with plant ID and Date as random effects. We assessed the relationship between J_{max} and V_{cmax} using linear regression. We analyzed carbon isotope ($\delta^{13}C$) values using ANOVA and estimated means and 95% confidence intervals using bootstrap sampling. We conducted post-hoc pairwise comparisons using Tukey's HSD.

We fit models using the lme4 package (Bates et al., 2015) and obtained p-values and statistical summaries via lmerTest (Kuznetsova et al., 2017). We calculated post-hoc comparisons and estimated marginal means using the emmeans package (Lenth, 2025) and conducted bootstrap analyses using the boot package (Davison &Hinkley, 1997; Canty & Ripley, 2024).

3. Results

3.1. Soil Moisture

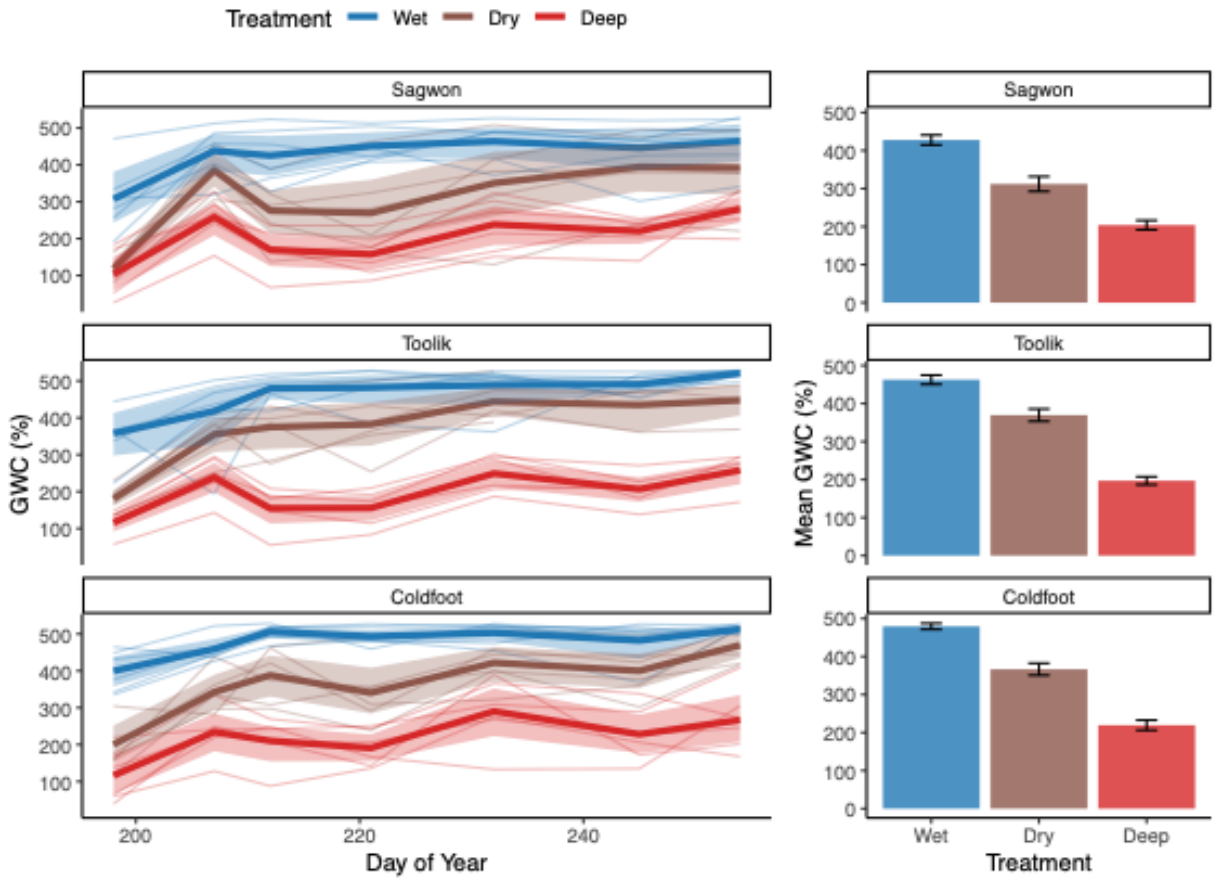

Figure 2. Soil gravimetric water content (GWC) as measured weekly through the duration of the experiment. (a-c) Seasonal patterns of soil GWC (%) across treatments (Wet, Dry, and Deep) at Sagwon, Toolik, and Coldfoot sites. Heavier lines show treatment means with 95% confidence intervals (shaded areas), while thin lines represent individual pots. (d-f) Mean GWC (%) (± SE) for each treatment by source population.

The three watering treatments successfully maintained distinct soil moisture levels throughout the experiment (Figure 2). Wet treatments maintained the highest gravimetric water content (GWC), averaging 456.7 ± 6.7%. Dry treatments reduced GWC by approximately 108% relative to Wet treatments, maintaining an average of 348.8 ± 10.2%. Deep treatments showed the lowest soil moisture, with GWC averaging 206.8 ± 7.0%, representing a reduction of 250% compared to Wet treatments.

A linear mixed-effects model confirmed the effectiveness of these treatments (GWC calculated as percentage on dry mass basis, tussock ID as random effect). The model revealed strong treatment effects on GWC ($p < 0.001$), with all treatments significantly differing from each other ($p < 0.001$ for all pairwise comparisons). Population showed a marginal effect on GWC ($p = 0.053$), with Coldfoot tending to have slightly higher moisture levels compared to Sagwon and Toolik. There was no significant Treatment × Population interaction ($p = 0.615$), indicating uniform treatment effect across source populations.

3.2. *Leaf-Level Phenology*

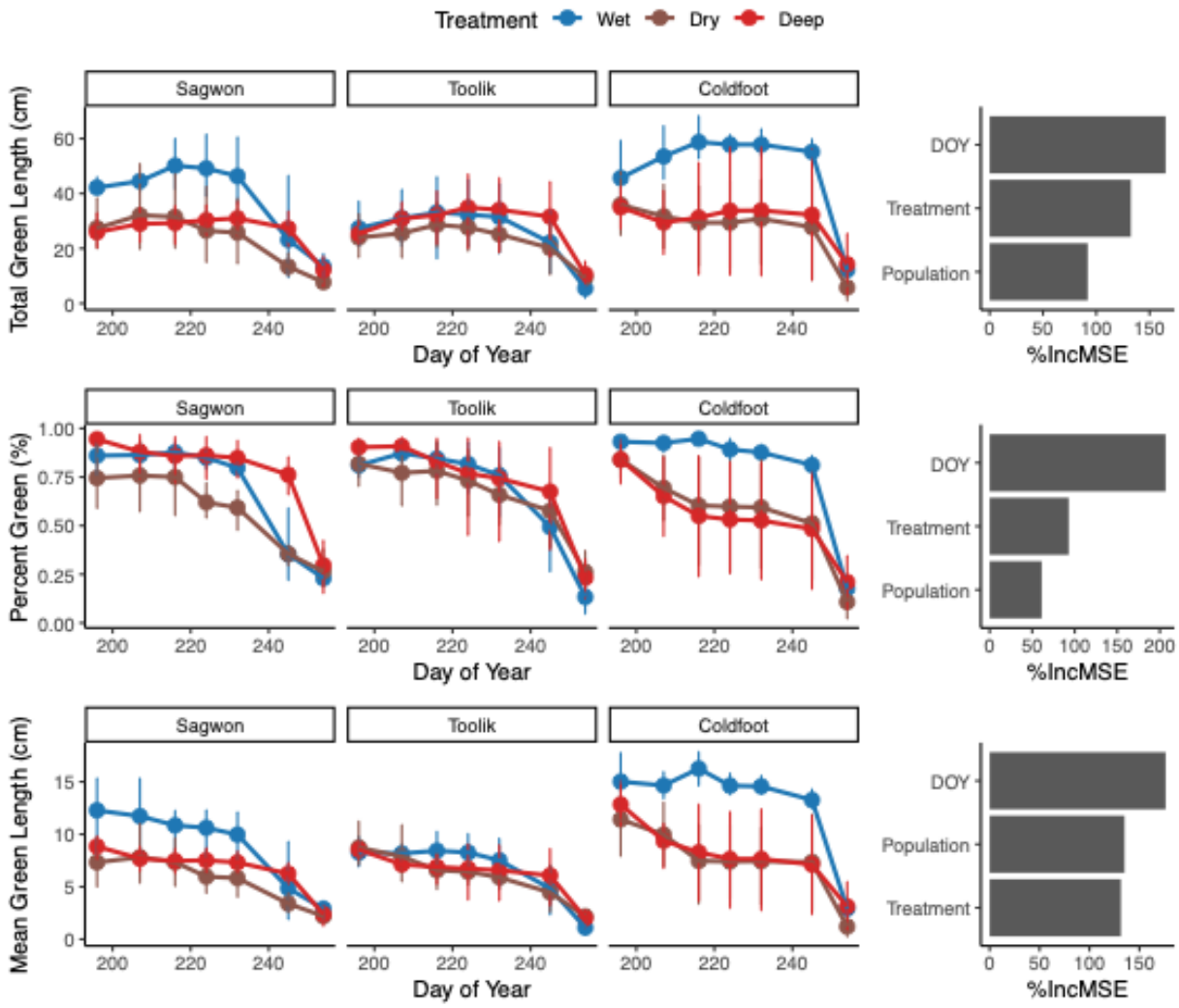

Figure 3. Growth and senescence metrics of *E. vaginatum* from three populations (Sagwon, Toolik, and Coldfoot) grown under different watering treatments in a common garden experiment. *Top:* Total green leaf

length per tiller, *Middle:* green tissue length as a percentage of total tiller length, and *Bottom:* average green leaf length per tiller measured throughout the growing season. Points represent means ± 95% confidence intervals (n = 6 per treatment). Right panels display random forest variable importance plots, where %IncMSE metric indicates each variable's relative importance in the model.

Leaf phenology metrics, including tiller total green length, average green leaf length, and percent green, exhibited significant declines over the growing season (DOY) across all treatments and populations (Figure 3; Table S1). The effect of DOY was highly significant for all three metrics (tiller total green length, percent green, and average green leaf length: all $p < 0.001$), indicating a strong seasonal decline in leaf greenness and length.

Treatment effects varied among the different metrics. Average green leaf length showed significant main effects of both Treatment ($p = 0.004$) and Population ($p = 0.002$). Tiller total green length showed a significant main effect of Treatment ($p = 0.034$) but not Population ($p = 0.117$), while percent green showed no significant main effects of either Treatment ($p = 0.212$) or Population ($p = 0.673$). The Treatment × Population interaction was not significant for any metric (tiller total green length: $p = 0.335$; percent green: $p = 0.253$; average green leaf length: $p = 0.152$), suggesting that populations responded similarly to the drying treatments overall.

There was a significant interaction between Treatment and DOY for all three phenology metrics (tiller total green length: $p < 0.001$; percent green: $p < 0.001$; average green leaf length: $p < 0.001$; Table S1), indicating that drying treatments altered the rate and timing of seasonal decline. This interaction was particularly strong for tiller total green length, where both drying treatments showed accelerated declines compared to control conditions (Deep × DOY: estimate = -75.80 ± 34.95, $p = 0.031$; Dry × DOY: estimate = -120.31 ± 38.28, $p = 0.002$).

The control (Wet) treatment maintained higher green leaf length and percentage of green tissue across the season at all populations compared to the drying treatments. For the Coldfoot population, tiller total green length in the control treatment remained stable until late in the season (DOY ~ 230), after which a gradual decline occurred. In contrast, both Deep and Dry treatments exhibited an earlier decline in green leaf length, particularly for Coldfoot and Sagwon populations. By DOY ~ 220, Coldfoot and Sagwon plants in the Deep and Dry treatments had already lost a substantial portion of their green tissue, whereas control plants maintained higher green tissue levels over the same period.

For the percent green metric, there were no significant main effects of treatment or population, but a significant Treatment × DOY interaction ($p < 0.001$) suggests that drying treatments influenced the timing and rate of senescence rather than overall green tissue maintenance. For tiller total green length, both Deep and Dry treatments showed significant interactions with DOY (Deep × DOY: $p = 0.031$; Dry × DOY: $p = 0.002$), indicating accelerated seasonal decline compared to control conditions.

Random forest models explained 32-47% of the variance in leaf phenology metrics (average green leaf length: 46.5%, percent green: 43.2%, total green length: 32.4%). For all three metrics, DOY was the strongest predictor of phenological change, as indicated by both percent increase in mean squared error (%IncMSE) and node purity measures. Treatment importance was comparable to population effects for average green leaf length (%IncMSE: 131.5 vs 135.1), but had stronger relative importance for percent green (%IncMSE: 93.0 vs 61.2) and total green length (%IncMSE: 132.4 vs 92.0). These results align with the linear model findings, confirming the primary importance of seasonal timing (DOY) in driving phenological patterns, while also highlighting substantial treatment effects that modify these seasonal patterns.

3.3. Whole-plant phenology

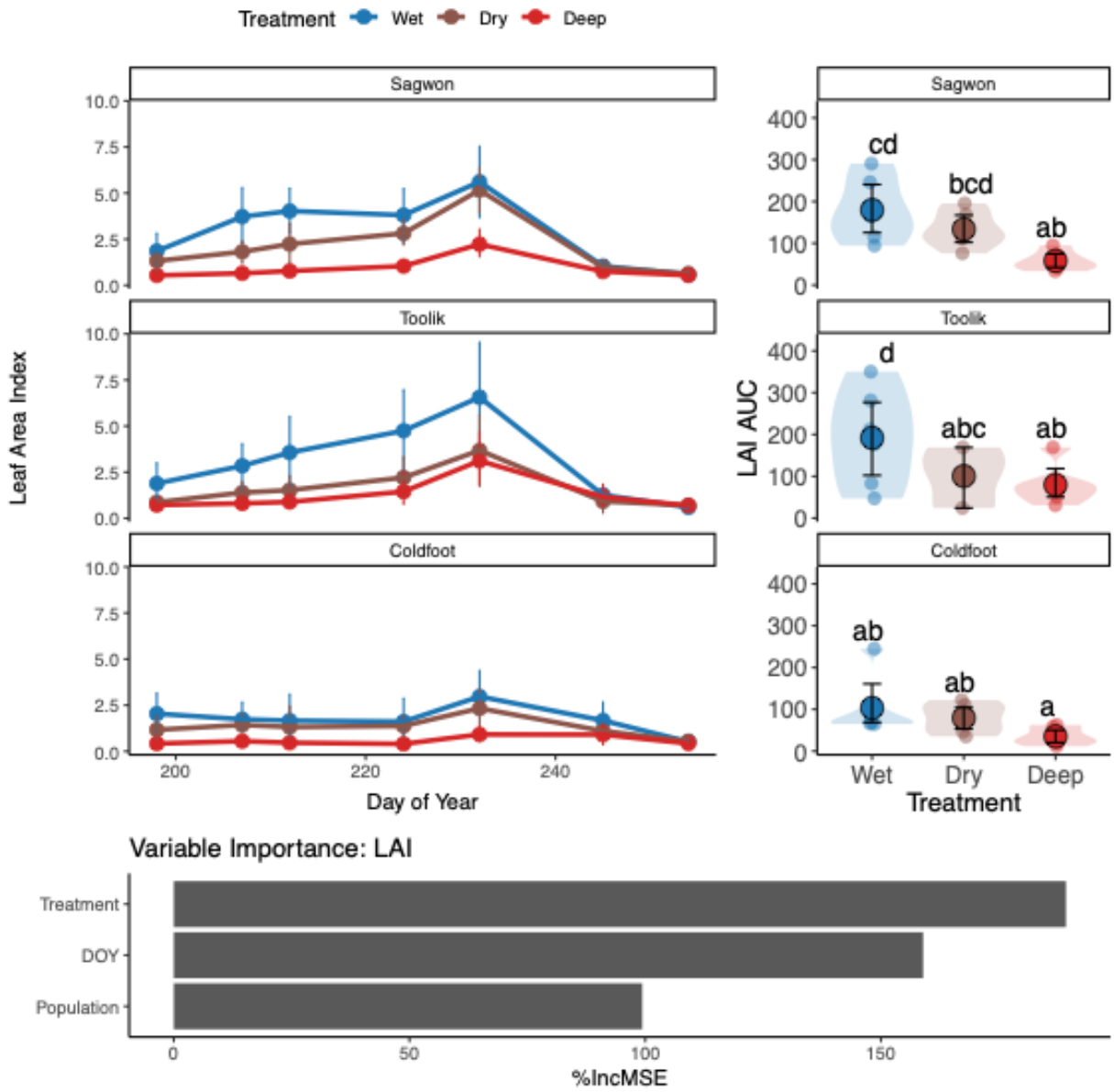

Figure 4. Leaf area index (LAI) dynamics and cumulative seasonal leaf area production for *E. vaginatum* populations (Sagwon, Toolik, and Coldfoot) under three watering treatments in a common garden study. *Top left:* Time-series plots of LAI throughout the growing season, with points showing means ± 95% confidence intervals. *Top right:* Violin plots of area under the curve (AUC) for LAI, representing total seasonal leaf area production. Jittered points show individual values, and large circles with error bars indicate estimated marginal means with 95% confidence intervals. Letter *annotations* above each group indicate significant differences among treatment × population combinations, derived from a quadratic linear mixed-effects model (LME) applied to the longitudinal time-series data ($p < 0.05$). *Bottom:* Random Forest variable importance plots, with bars ranked by the %IncMSE metric to indicate predictor importance.

Leaf area index (LAI) exhibited a strong quadratic response to day of year, indicating a hump-shaped seasonal trajectory with a peak mid-season followed by a decline in late summer (Figure 4; Table S2). This pattern reflects the typical phenology of *Eriophorum vaginatum*, with leaf elongation and canopy development occurring early in the season, followed by leaf senescence later in the growing season. The effect of DOY was highly significant ($p < 0.001$), capturing the non-linear seasonal dynamics.

Both drying treatments had negative effects on LAI compared to the wet treatment, though the magnitude varied. While the drying-only treatment showed a non-significant reduction in LAI (estimate = -0.82, $p = 0.162$), the deep drying treatment significantly reduced LAI (estimate = -2.02, $p = 0.001$). These results suggest that deeper soil drainage has more profound consequences for tussock growth than surface-level drying alone. There were also significant population effects ($p = 0.030$), with the Coldfoot population showing lower LAI overall (estimate = -1.21, $p = 0.041$) compared to other populations.

The interaction between DOY and treatment was significant ($p < 0.001$), indicating that seasonal patterns of LAI development differed among treatments. Additionally, there was a significant DOY × Population interaction ($p < 0.001$), suggesting population-specific seasonal trajectories. However, the Treatment × Population interaction was not significant ($p = 0.665$), indicating that populations responded similarly to the drying treatments despite their different seasonal patterns. These results suggest that while populations maintain distinct phenological patterns and treatments affect seasonal LAI development, the population-level responses to drying treatments are consistent across populations.

Similar seasonal and treatment effects were observed for NDVI and biomass (Figure S3, S4), with deep drying significantly reducing both metrics. Population effects were strongest for LAI, while biomass showed a marginal population effect

Random forest models explained 40.4% of the variance in LAI patterns. Treatment was the strongest predictor of LAI variation (%IncMSE = 189.1), followed by DOY (%IncMSE = 158.1) and population (%IncMSE = 99.9). This analysis supports the linear model findings while highlighting the relative importance of treatment effects on LAI, suggesting that experimental manipulations of soil moisture had stronger effects on canopy development than either seasonal timing or population identity.

3.4. Leaf Water Potential

A two-way ANOVA was conducted to evaluate the effects of population, treatment, and their interaction on leaf water potential. The analysis revealed no significant main effect of population on water potential ($p = 0.984$) or treatment ($p = 0.229$). Additionally, the interaction between population and treatment was not significant ($p = 0.568$). While no main effects reached significance, treatment effects did exhibit marginal trends across treatments.

Mean water potential values ranged from -1.14 ± 0.12 MPa (Toolik-Dry) to -1.40 ± 0.11 MPa (Sagwon-Deep) across treatments and populations (Figure 5). Post-hoc pairwise comparisons using estimated marginal means confirmed that no significant pairwise differences were detected between populations or treatments after adjusting for multiple comparisons (all $p > 0.05$). The lack of significant interaction suggests that treatment effects on water potential were consistent across populations.

It is important to note that only healthy leaves were selected for measurement, with visibly senesced or senescing leaves excluded from sampling. This sampling approach may have contributed to the observed lack of significant differences, as plants likely maintained their leaf water potential within a narrow range to prevent physiological damage. More severely stressed leaves may have senesced or dropped prior to measurement, leaving surviving leaves with similar water potential values across populations and treatments.

3.5. Maximum Photosynthetic Rate

Eighty measurements were made over three days, with some repeated measurements of individual tussocks. For A_{max} there was a significant main effect of treatment ($p = 0.002$), with the strongest effects seen in the Deep treatment, which significantly reduced photosynthetic capacity compared to the Wet control (estimate = -5.65 ± 1.74, $p = 0.003$). The Coldfoot population showed significantly lower A_{max} compared to Sagwon (estimate = -4.71 ± 1.70, $p = 0.009$), representing reduced photosynthesis in the southernmost compared to northernmost population. Population effects overall were marginally non-significant ($p = 0.082$), and no significant interaction was detected between population and treatment ($p = 0.431$), suggesting

that treatment effects on photosynthesis were consistent across populations despite baseline differences.

Stomatal conductance (g_s) showed a significant main effect of treatment ($p = 0.010$), with significant effects only detected in the Deep treatment, which showed reduced conductance compared to the Wet control (estimate = -0.169 ± 0.063, $p = 0.012$). Neither population ($p = 0.687$) nor the interaction between population and treatment ($p = 0.571$) significantly influenced g_s, indicating consistent stomatal responses to water stress across populations.

For C_i (Supplemental Figure S3), no significant effects were detected for population ($p = 0.425$), treatment ($p = 0.399$), or their interaction ($p = 0.998$). The lack of treatment effects on C_i (Figure S5), despite reduced stomatal conductance, suggests coordinated regulation of CO_2 supply and demand under drought conditions.

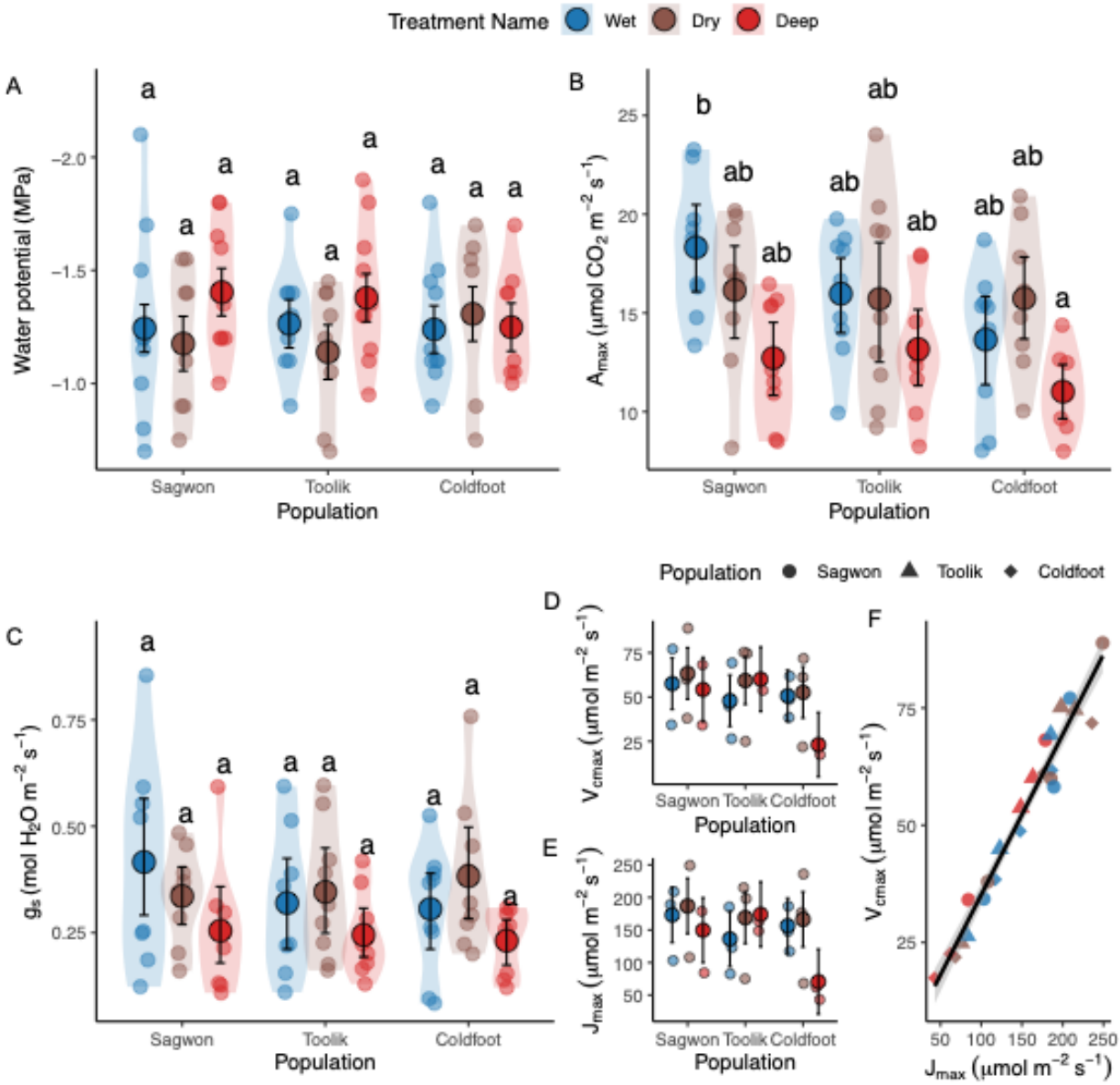

Figure 5. Physiological responses of *E. vaginatum* from three populations (Sagwon, Toolik, and Coldfoot) to experimental water treatments in a common garden study. (A) Midday leaf water potential (MPa, displayed on a reversed y-axis to reflect increasing water stress with more negative values); (B) maximum photosynthetic rate (Amax); (C) stomatal conductance (g_s); (D-F) biochemical parameters derived from A-Ci curves, showing (D) maximum carboxylation rate (V_{cmax}), (E) maximum electron transport rate (J_{max}), and (F) the relationship between J_{max} and V_{cmax}. In panels A-C, violin plots show the distribution of raw data, with individual measurements (jittered points), estimated marginal means from mixed-effects models (large filled circles) and

their 95% confidence intervals (error bars). In panels D-E, points show individual measurements, large filled circles show estimated marginal means with 95% confidence intervals. Panel F shows individual measurements by population (shapes) and treatment (colors), with the black line showing the linear regression with 95% confidence interval (shaded area). Different letters indicate significant differences between treatment × population combinations based on pairwise comparisons with Tukey's adjustment ($p < 0.05$).

3.6. Biochemical photosynthetic parameters

Mixed-effects models for V_{cmax} and J_{max} examined the effects of Population and Treatment, with random intercepts for Plant ID and Date included in both models. For V_{cmax}, the variance for Plant ID was effectively zero, indicating a negligible impact. The fixed effects showed no significant interaction between Population and Treatment ($p = 0.695$), and Population ($p = 0.302$) and Treatment ($p = 0.548$) effects were not significant. Similarly, for J_{max} there were no significant effects of Population ($p = 0.399$), Treatment ($p = 0.403$), or their interaction ($p = 0.555$), although the random effect variance for Date was higher than for V_{cmax} (936.3 vs 43.38). Despite the lack of statistical significance, differences in mean V_{cmax} and J_{max} values were notable, particularly in the Coldfoot population under drying and deepening treatments. These variations suggest that environmental treatments may have influenced these parameters, but the small sample size ($n = 24$) may have limited the detection of significant effects. Additionally, a strong positive relationship was observed between V_{cmax} and J_{max} through a simple linear regression (Figure 5; $R^2 = 0.960$, slope = 2.81 ± 0.12), highlighting a close association between these two photosynthetic parameters.

3.7. *Intrinsic Water Use Efficiency*

The $\delta^{13}C$ values showed larger mean differences between populations than between treatments (Figure 6), though all comparisons had confidence intervals that included zero. For population-level analysis, mean $\delta^{13}C$ values ranged from -26.77‰ in Sagwon (SG) to -26.15‰ in Coldfoot (CF), with Toolik (TL) showing an intermediate value of -26.20‰. Population differences were moderate in magnitude, with the largest difference of 0.628‰ between Coldfoot and Sagwon (95% CI: -0.02‰ to 1.40‰), and a similar difference of 0.583‰ between Coldfoot and Toolik. In contrast, treatment effects were notably smaller, with mean $\delta^{13}C$ values differing by less than 0.4‰ across all treatments (Dry: -26.15‰, Wet: -26.31‰, Deep: -

26.55‰). ANOVA results confirmed the lack of significant differences across both populations ($p = 0.210$) and treatments ($p = 0.574$), with no significant interaction ($p = 0.796$).

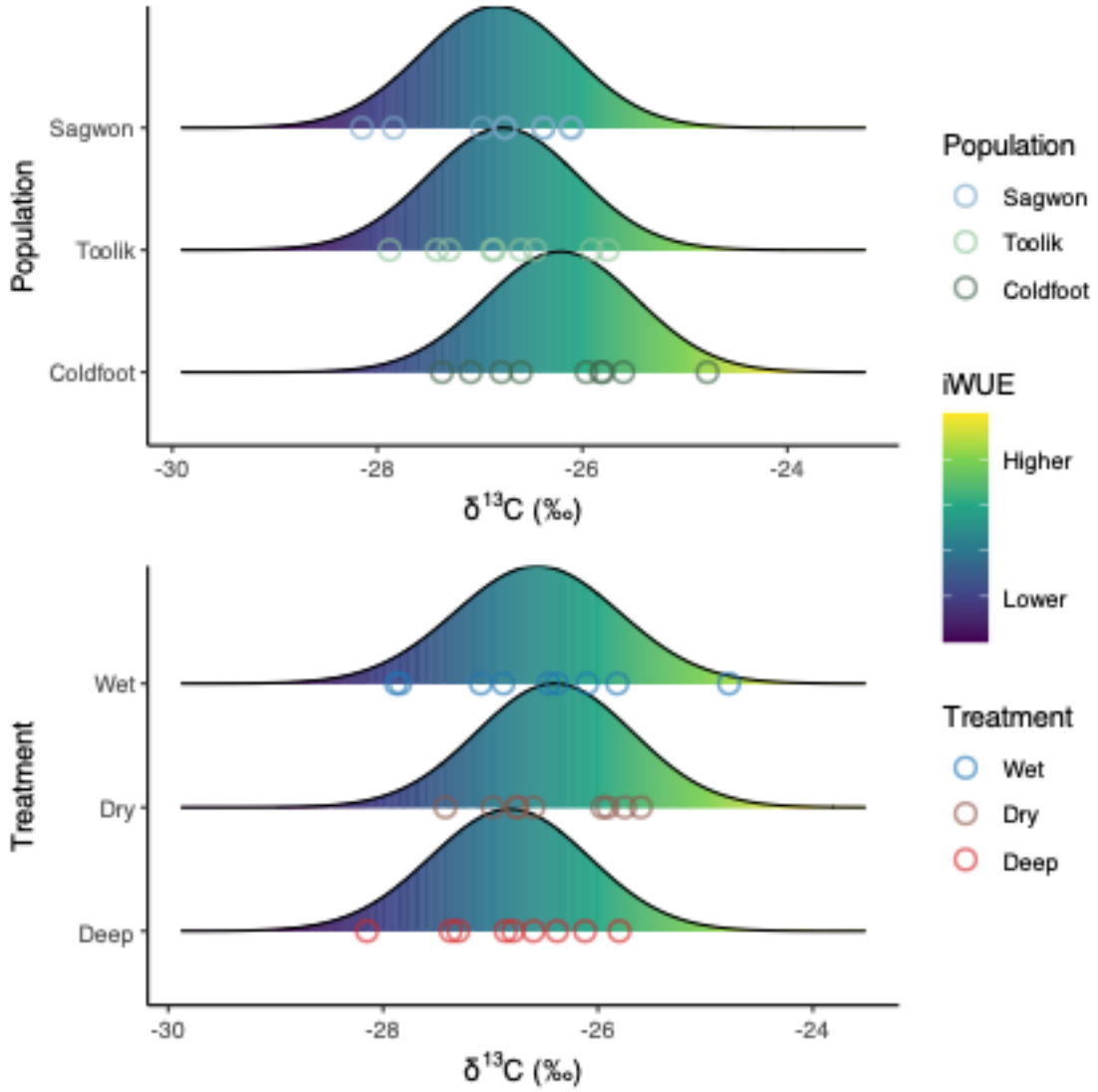

Figure 6. Carbon isotope composition ($\delta^{13}C$) of leaf tissue grown. *Top:* Distribution of $\delta^{13}C$ values across source populations (Sagwon, Toolik, and Coldfoot) and *bottom*: across watering treatments (Wet, Dry, Deep). In both panels, shaded ridgelines show the density distribution of bootstrapped means (n = 1000 bootstraps), gradient-filled where darker colors indicate less negative $\delta^{13}C$ values (corresponding to higher intrinsic water use efficiency, iWUE). Individual measurements are shown as points, shaped as circles with colored outlines.

4. Discussion

Our results demonstrate that soil moisture availability critically drives plant phenology, physiology, and productivity in Arctic tundra ecosystems, with notable differences in responses across biological scales—from individual leaves to whole plants. Plants exposed to drying treatments exhibited earlier senescence, reduced photosynthetic capacity (A_{max}), and lower cumulative leaf area index (LAI) compared to wet controls, with the deep drying treatment—simulating active layer deepening—showing the most severe impacts. Population-level differences were evident, with the southern population (Coldfoot) showing lower physiological performance under drought compared to northern populations (Sagwon and Toolik), indicating that local adaptation to moisture regimes influences plant responses to climate change (Peterson et al., 2012).

4.1. Scale-Dependent Plasticity in Drought Responses

Our findings reveal a scale-dependent hierarchy of drought responses in *Eriophorum vaginatum*. At the leaf level, limited plasticity was evident, as water potential, stomatal conductance, and leaf tissue greenness remained consistent across treatments and populations, indicating a binary response—leaves were either functional or senesced under stress. At the tiller level, plants exhibited moderate plasticity by adjusting leaf number and size to balance water retention and photosynthetic capacity. Average green leaf length—a function of both leaf elongation and retention—was influenced by both treatment and population, reflecting a more nuanced response to water stress. At the canopy level, the most plastic adjustments occurred, as plants reduced overall LAI with increasing drought severity.

Our drying treatments had pronounced effects on plant phenology across all populations, with impacts varying by both drying severity and ecotype. The deep drying treatment produced the most substantial reductions in LAI and green leaf length compared to surface-level drying, while the wet treatment maintained higher green leaf length and percent green tissue throughout the growing season. This performance under saturated conditions aligns with historical observations by Gore & Urquhart (1966), who demonstrated that *E. vaginatum* performs best in waterlogged conditions due to its ability to exploit nutrients in saturated soils.

The timing of phenological declines varied across treatments and populations. Although senescence timing in *E. vaginatum* is greatly influenced by genetic factors—where southern

ecotypes, adapted to longer growing seasons, generally exhibit delayed senescence compared to northern ecotypes (Parker et al., 2017, 2021)—our findings suggest that severe moisture stress can override genetic controls. Green leaf length declined earlier in both the deep and dry treatments, with the Coldfoot population showing the steepest decline despite its southern origin. This pattern suggests that environmental stress can accelerate senescence, potentially shortening growing seasons and diminishing ecosystem productivity (Zona et al., 2022).

4.2. Strategies for Water Balance and Carbon Uptake

Under well-watered conditions, we observed A_{max} values (13.7-18.4 μmol m^{-2} s^{-1}) comparable to previous measurements at Toolik (Souther et al., 2014), with the northern Sagwon population showing unexpectedly high photosynthetic capacity (18.4 μmol m^{-2} s^{-1}). Deep drying reduced A_{max} in all populations (11.3-13.3 μmol m^{-2} s^{-1}), supporting previous findings about water stress impacts on photosynthetic uptake across ecotypes (Keane et al., 2021). The observed J_{max}/V_{cmax} ratio of 2.81 roughly aligns with the high ratio (2.09) previously reported by Schedlbauer et al. (2018), suggesting *E. vaginatum* invests heavily in electron transport relative to Rubisco carboxylation to maximize photosynthesis during short, light-rich growing seasons.

The physiological responses highlight complex water management mechanisms. Plants maintained leaf water potential and intrinsic water use efficiency (IWUE) within a narrow range across treatments and populations, likely a critical survival strategy where water availability can fluctuate dramatically (Oberbauer & Miller, 1981; Stoner & Miller, 1975). Although the differences in IWUE were not significant, the trend is consistent with reduced stomatal density for the southern populations (Peterson et al., 2012). The observed leaf water potentials (-1.1 to -1.4 MPa) approached critical thresholds (-1.2 to -1.5 me.MPa) identified by (Oberbauer & Miller, 1982) where drought stress severely limits photosynthetic capacity. The lack of significant IWUE differences across treatments suggests that rather than fully closing stomata, plants maintained moderate stomatal conductance, allowing for continued photosynthesis at reduced rates. This aligns with previous research indicating that *Eriophorum vaginatum* exhibits partial stomatal regulation in response to atmospheric water stress, rather than complete closure leading to increased IWUE (Blanken & Rouse, 1996; Gebauer et al., 1998). The decline in A_{max} under drying treatments suggests a reduction in photosynthetic capacity that is not driven by either stomatal closure or direct biochemical inhibition. Given the stable J_{max} and Vc_{max}, this

decline may be due to mesophyll conductance limitations or metabolic downregulation in response to water stress, with plants maintaining moderate stomatal conductance but reduced carbon assimilation as a protective strategy (Gebauer et al., 1998; Sáez et al., 2018; Souther et al., 2014); however, this should be confirmed with more targeted future research.

Structural traits further influence plant water relations. While deeper drying had more pronounced effects on LAI and green leaf length than surface drying, the ability of in-situ rooting depth to track thaw depth remains uncertain. *E. vaginatum*'s annual root growth pattern (Wein, 1973) combined with root growth lagging leaf development by approximately 28 days (Ma, Parker, Fetcher, et al., 2022), may increase vulnerability to early-season water availability changes from deeper permafrost thaw. Root pruning decreased growth of several species including *E. vaginatum* (Oberbauer & Miller, 1982). The relationship of root growth to soil condition highlights root architecture's role in moisture responses, with more extensive root systems potentially better equipped for deep soil drying (Blanken & Rouse, 1996; Caldwell et al., 1978). While our study did not measure belowground biomass, previous research on Arctic species shows increased root-to-shoot ratios under drought stress (Landhäusser et al., 1996).

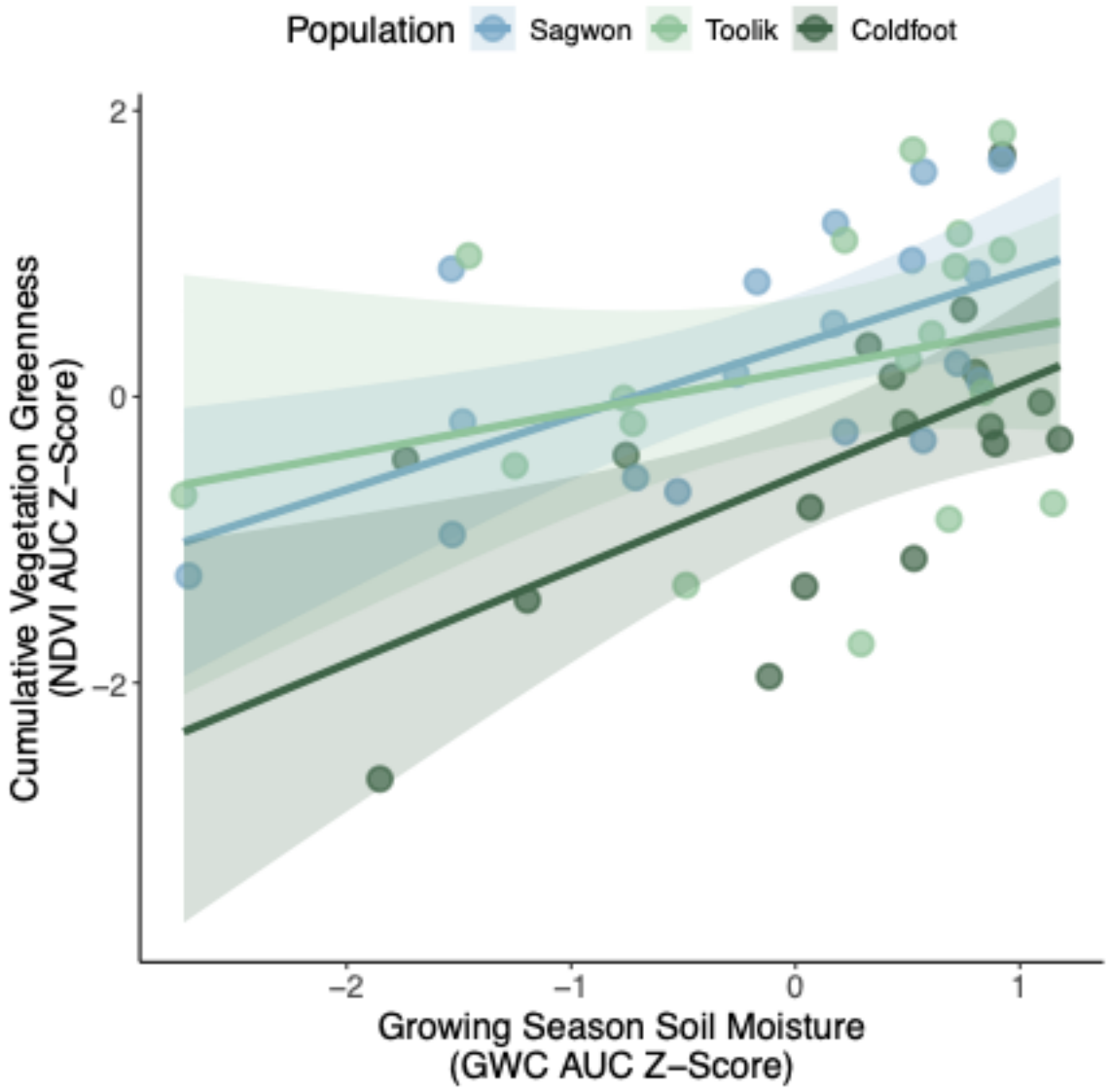

Figure 7. Relationship between standardized (z-score) values of growing season soil moisture (quantified as area under the curve [AUC] of gravimetric water content [GWC]) and cumulative vegetation greenness (NDVI AUC) tussocks from each of three populations. Points represent individual plants, with colors indicating source population. Lines show population-specific linear regressions with 95% confidence intervals (shaded areas).

4.3. Local Adaptation and Vulnerability in a Changing Environment

Our results demonstrate that soil moisture can control *E. vaginatum*, with all populations showing clear responses to moisture availability (Figure 7). Although we found no significant Population × Treatment interactions (Figure S6), baseline differences in physiological and structural traits suggest population-specific vulnerability exists even in the absence of

population-specific responses to stress. The southernmost Coldfoot population exhibited lower photosynthetic capacity and canopy productivity relative to northern populations, indicating these plants may operate closer to hydraulic failure thresholds even under favorable conditions. While all populations experienced similar declines in photosynthesis and canopy size under drying treatments, Coldfoot's lower baseline performance points to a heightened risk of long-term declines.

Local adaptation often creates ecotypes that are highly specialized for their current environments but potentially maladaptive under new conditions (Hereford, 2009; Hufford & Mazer, 2003). While species might be expected to simply track their preferred conditions northward under climate change, successful establishment can be limited by adaptational lag - the mismatch between current genotypes and rapidly changing environments (Hoffmann & Sgrò, 2011; Jump & Peñuelas, 2005). This framework helps explain why the southern Coldfoot population, adapted to historically wetter conditions, shows greater vulnerability to drying stress, a pattern consistent with broader findings about ecotype-specific responses to climate extremes (Beierkuhnlein et al., 2011). On the other hand, the greater sensitivity of the Coldfoot population may also be explained in part by its taller stature, as Olson et al. (2018) demonstrated that taller plants with wider conduits are more susceptible to hydraulic failure under water stress.

4.4. Implications for Tundra Ecosystems and the Arctic

The observed reductions in LAI and earlier senescence under drying treatments suggest that *E. vaginatum* productivity may decline as soil moisture becomes limited, potentially reducing Arctic tundra carbon sequestration capacity (Euskirchen et al., 2012; Natali et al., 2015). These changes in canopy development could affect ecosystem energy balance through reduced evaporative cooling (Rietze et al., 2024). Since Arctic ecosystems store a large proportion of the world's soil carbon, any reduction in plant productivity and carbon uptake could contribute to a feedback loop that accelerates climate warming (Andresen et al., 2020; Zona et al., 2022).

The population-level differences highlight potential shifts in plant community composition under changing climatic conditions. Southern populations, which appear to be more vulnerable to drying stress, may face greater challenges than northern populations, with population shifts leading to changes in community structure and ecosystem processes (Curasi et al., 2022, 2019; Greenup, 2000; Scharn et al., 2021). Latitudinal migration of populations may be constrained by

both genetic and environmental barriers, particularly at the treeline (Stunz et al., 2022) and future adaptation to changing Arctic conditions may depend more on phenotypic plasticity or novel adaptations within existing populations than on migration.

5. Conclusions

Our findings underscore how soil moisture variability shapes Arctic plant phenology, physiology, and productivity through scale-dependent responses that vary from leaf to canopy levels. The combination of reduced leaf area and reduced carbon uptake per unit leaf area could substantially diminish productivity and viability of *E. vaginatum* under drought stress, particularly concerning given the significant role of the plant in maintaining Arctic ecosystem structure and carbon stocks (Curasi et al., 2022)

While southern populations are genetically programmed for longer growing seasons (Parker et al., 2021), moisture stress can override these patterns, triggering earlier senescence and reduced productivity. The relative conservation of physiological traits like leaf water potential and water use efficiency across populations suggests fundamental constraints on drought adaptation, while baseline differences in performance indicate population-specific vulnerabilities may exist even without population-specific stress responses. Our findings align with the idea that drought-induced senescence serves as a protective response to limit water loss and balance resource demand (Sade et al., 2018), though the exact triggers and controls of this process remain uncertain.

Though our treatments focused on soil moisture manipulation, the observed responses may be broadly applicable across the Arctic as increases in atmospheric evaporative demand are projected to be widespread (Grossiord et al., 2020; Sulman et al., 2016). Ultimately, our findings highlight the need to consider spatial and temporal variations in soil moisture, and to consider water balance as resource or as stressor (Kemppinen et al., 2019), when predicting Arctic plant responses under climate change. The reduced growth and carbon uptake we observed demonstrates how changing moisture regimes could alter the environmental fit and ecological function of this foundational species, with substantial consequences for ecosystem structure and carbon balance in the future Arctic.

References

A. C. Davison, & D. V. Hinkley. (1997). *Bootstrap Methods and Their Applications*. Cambridge University Press.

Andresen, C. G., Lawrence, D. M., Wilson, C. J., McGuire, A. D., Koven, C., Schaefer, K., Jafarov, E., Peng, S., Chen, X., Gouttevin, I., Burke, E., Chadburn, S., Ji, D., Chen, G., Hayes, D., & Zhang, W. (2020). Soil moisture and hydrology projections of the permafrost region – a model intercomparison. *The Cryosphere*, *14*(2), 445–459.

Angelo Canty, & B. D. Ripley. (2024). *boot: Bootstrap R (S-Plus) Functions*.

Bates, D., Mächler, M., Bolker, B., & Walker, S. (2015). Fitting Linear Mixed-Effects Models Using \textbflme4. *Journal of Statistical Software*, *67*(1). https://doi.org/10.18637/jss.v067.i01

Beierkuhnlein, C., Thiel, D., Jentsch, A., Willner, E., & Kreyling, J. (2011). Ecotypes of European grass species respond differently to warming and extreme drought. *Journal of Ecology*, *99*(3), 703–713.

Bennington, C. C., Fetcher, N., Vavrek, M. C., Shaver, G. R., Cummings, K. J., & McGraw, J. B. (2012). Home site advantage in two long-lived arctic plant species: results from two 30-year reciprocal transplant studies. *The Journal of Ecology*, *100*(4), 841–851.

Berner, L. T., Jantz, P., Tape, K. D., & Goetz, S. J. (2018). Tundra plant above-ground biomass and shrub dominance mapped across the North Slope of Alaska. *Environmental Research Letters*, *13*(3), 035002.

Black, K. L., Wallace, C. A., & Baltzer, J. L. (2021). Seasonal thaw and landscape position determine foliar functional traits and whole-plant water use in tall shrubs on the low arctic tundra. *The New Phytologist*, *231*(1), 94–107.

Blanken, P., & Rouse, W. (1996). Evidence of water conservation mechanisms in several subarctic wetland species. *Journal of Applied Ecology*, *33*, 842–850.

Borchers, H. W. (2023). *Practical Numerical Math Functions [R package pracma version 2.4.4]*. https://CRAN.R-project.org/package=pracma

Caldwell, M. M., Johnson, D. A., & Fareed, M. (1978). Constraints on tundra productivity: Photosynthetic capacity in relation to solar radiation utilization and water stress in arctic and alpine tundras. In *Ecological Studies* (pp. 323–342). Springer New York.

636 Chandler, J. L., McGraw, J. B., Bennington, C., Shaver, G. R., Vavrek, M. C., & Fetcher, N.
637 (2015). Tiller population dynamics of reciprocally transplanted *Eriophorum vaginatum* L.
638 ecotypes in a changing climate. *Population Ecology*, *57*(1), 117–126.
639 Chapin, F. S., III, Fetcher, N., Kielland, K., Everett, K. R., & Linkins, A. E. (1988). Productivity
640 and nutrient cycling of Alaskan tundra: Enhancement by flowing soil water. *Ecology*,
641 *69*(3), 693–702.
642 Chapin, F. S., van Cleve, K., & Chapin, M. C. (1979). Soil Temperature and Nutrient Cycling in
643 the Tussock Growth Form of Eriophorum Vaginatum. *The Journal of Ecology*, *67*(1),
644 169–189.
645 Chapin F. Stuart, & Shaver Gaius R. (1985). Individualistic Growth Response of Tundra Plant
646 Species to Environmental Manipulations in the Field. *Ecology*, *66*(2), 564–576.
647 Chivers, M. R., Turetsky, M. R., Waddington, J. M., Harden, J. W., & McGuire, A. D. (2009).
648 Effects of Experimental Water Table and Temperature Manipulations on Ecosystem CO2
649 Fluxes in an Alaskan Rich Fen. *Ecosystems* , *12*(8), 1329–1342.
650 Curasi, S. R., Fetcher, N., Hewitt, R. E., Lafleur, P. M., Loranty, M. M., Mack, M. C., May, J.
651 L., Myers-Smith, I. H., Natali, S. M., Oberbauer, S. F., Parker, T. C., Sonnentag, O.,
652 Vargas Zesati, S. A., Wullschleger, S. D., & Rocha, A. V. (2022). Range shifts in a
653 foundation sedge potentially induce large Arctic ecosystem carbon losses and gains.
654 *Environmental Research Letters*, *17*(4), 045024.
655 Curasi, S. R., Parker, T. C., Rocha, A. V., Moody, M. L., Tang, J., & Fetcher, N. (2019).
656 Differential responses of ecotypes to climate in a ubiquitous Arctic sedge: implications
657 for future ecosystem C cycling. *The New Phytologist*, *223*(1), 180–192.
658 Duursma, R. A. (2015). Plantecophys--an R package for analysing and modelling leaf gas
659 exchange data. *PloS One*, *10*(11), e0143346.
660 Euskirchen, E. S., Bret-Harte, M. S., Scott, G. J., & Edgar, C. (n.d.). *Seasonal patterns of carbon*
661 *dioxide and water fluxes in three representative tundra ecosystems in northern Alaska*.
662 https://doi.org/10.1890/ES11-00202.1
663 Farquhar, G. D., Caemmerer, S. von, & Berry, J. A. (1980). A biochemical model of
664 photosynthetic CO2 assimilation in leaves of C3 species. *Planta*, *149*(1), 78–90.

665 Farquhar, G. D., Ehleringer, J. R., & Hubick, K. T. (1989). Carbon isotope discrimination and
666 photosynthesis. *Annual Review of Plant Physiology and Plant Molecular Biology*, *40*(1),
667 503–537.
668 Fetcher, N., & Shaver, G. R. (1990). Environmental Sensitivity of Ecotypes as a Potential
669 Influence on Primary Productivity. *The American Naturalist*, *136*(1), 126–131.
670 Gebauer, R., Reynolds, J., & Tenhunen, J. (1998). Diurnal patterns of CO2 and H2O exchange of
671 the Arctic sedges Eriophorum angustifolium and E. vaginatum (Cyperaceae). *American*
672 *Journal of Botany*, *85*(4), 592.
673 Gore, A. J. P., & Urquhart, C. (1966). The Effects of Waterlogging on the Growth of Molinia
674 Caerulea and Eriophorum Vaginatum. *The Journal of Ecology*, *54*(3), 617.
675 Greenup, A. L. (2000). The role of Eriophorum vaginatum in CH4 flux from an ombrotrophic
676 peatland. *Plant and Soil*, *227*(1/2), 265–272.
677 Grossiord, C., Buckley, T. N., Cernusak, L. A., Novick, K. A., Poulter, B., Siegwolf, R. T. W.,
678 Sperry, J. S., & McDowell, N. G. (2020). Plant responses to rising vapor pressure deficit.
679 *The New Phytologist*, *226*(6), 1550–1566.
680 Hereford, J. (2009). A quantitative survey of local adaptation and fitness trade-offs. *The*
681 *American Naturalist*, *173*(5), 579–588.
682 Hoffmann, A. A., & Sgrò, C. M. (2011). Climate change and evolutionary adaptation. *Nature*,
683 *470*(7335), 479–485.
684 Hufford, K. M., & Mazer, S. J. (2003). Plant ecotypes: genetic differentiation in the age of
685 ecological restoration. *Trends in Ecology & Evolution*, *18*(3), 147–155.
686 Jorgenson, M. T., Racine, C. H., Walters, J. C., & Osterkamp, T. E. (2001). Permafrost
687 Degradation and Ecological Changes Associated with a WarmingClimate in Central
688 Alaska. *Climatic Change*, *48*(4), 551–579.
689 Jump, A. S., & Peñuelas, J. (2005). Running to stand still: adaptation and the response of plants
690 to rapid climate change. *Ecology Letters*, *8*(9), 1010–1020.
691 Keane, J. B., Toet, S., Ineson, P., Weslien, P., Stockdale, J. E., & Klemedtsson, L. (2021).
692 Carbon dioxide and methane flux response and recovery from drought in a hemiboreal
693 ombrotrophic fen. *Frontiers in Earth Science*, *8*.
694 https://doi.org/10.3389/feart.2020.562401

Kemppinen, J., Niittynen, P., Aalto, J., le Roux, P. C., & Luoto, M. (2019). Water as a resource, stress and disturbance shaping tundra vegetation. *Oikos (Copenhagen, Denmark)*, *128*(6), 811–822.

Kuznetsova, A., Brockhoff, P. B., & Christensen, R. H. B. (2017). lmerTest Package: Tests in Linear Mixed Effects Models. In *Journal of Statistical Software* (Vol. 82, Issue 13, pp. 1–26). https://doi.org/10.18637/jss.v082.i13

Landhäusser, S. M., Wein, R. W., & Lange, P. (1996). Gas exchange and growth of three arctic tree-line tree species under different soil temperature and drought preconditioning regimes. *Canadian Journal of Botany. Journal Canadien de Botanique*, *74*(5), 686–693.

Lara, M. J., Nitze, I., Grosse, G., Martin, P., & McGuire, A. D. (2018). Reduced arctic tundra productivity linked with landform and climate change interactions. *Scientific Reports*, *8*(1), 2345.

Lawrence, D. M., Koven, C. D., Swenson, S. C., Riley, W. J., & Slater, A. G. (2015). Permafrost thaw and resulting soil moisture changes regulate projected high-latitude CO 2 and CH 4 emissions. *Environmental Research Letters: ERL [Web Site]*, *10*(9), 094011.

Lenth, R. V. (2025). *emmeans: Estimated Marginal Means, aka Least-Squares Means*. https://rvlenth.github.io/emmeans/

Liaw, A., & Wiener, M. (2002). Classification and Regression by randomForest. In *R News* (Vol. 2, Issue 3, pp. 18–22). https://CRAN.R-project.org/doc/Rnews/

Ma, T., Parker, T., Fetcher, N., Unger, S. L., Gewirtzman, J., Moody, M. L., & Tang, J. (2022). Leaf and root phenology and biomass of Eriophorum vaginatum in response to warming in the Arctic. *Journal of Plant Ecology*, *15*(5), 1091–1105.

Ma, T., Parker, T., Unger, S., Gewirtzman, J., Fetcher, N., Moody, M. L., & Tang, J. (2022). Responses of root phenology in ecotypes of Eriophorum vaginatum to transplantation and warming in the Arctic. *The Science of the Total Environment*, *805*, 149926.

Mark, A. F., Fetcher, N., Shaver, G. R., & Chapin, F. S. (1985). Estimated Ages of Mature Tussocks of Eriophorum vaginatum along a Latitudinal Gradient in Central Alaska, U.S.A. *Arctic and Alpine Research*, *17*(1), 1–5.

McGraw, J. B., Turner, J. B., Souther, S., Bennington, C. C., Vavrek, M. C., Shaver, G. R., & Fetcher, N. (2015). Northward displacement of optimal climate conditions for ecotypes of

725 Eriophorum vaginatum L. across a latitudinal gradient in Alaska. *Global Change Biology*,
726 *21*(10), 3827–3835.
727 Natali Susan M., Schuur Edward A. G., Mauritz Marguerite, Schade John D., Celis Gerardo,
728 Crummer Kathryn G., Johnston Catherine, Krapek John, Pegoraro Elaine, Salmon Verity
729 G., & Webb Elizabeth E. (2015). Permafrost thaw and soil moisture driving CO2 and
730 CH4 release from upland tundra. *Journal of Geophysical Research: Biogeosciences*,
731 *120*(3), 525–537.
732 Oberbauer, S., & Miller, P. C. (1979). Plant water relations in Montane and tussock tundra
733 vegetation types in Alaska. *Arctic and Alpine Research*, *11*(1), 69–81.
734 Oberbauer, S., & Miller, P. C. (1981). Some aspects of plant water relations in Alaskan arctic
735 tundra species. *Arctic and Alpine Research*, *13*(2), 205–218.
736 Oberbauer, S., & Miller, P. C. (1982). Growth of Alaskan tundra plants in relation to water
737 potential. *Ecography*, *5*(2), 194–199.
738 Olson, M. E., Soriano, D., Rosell, J. A., Anfodillo, T., Donoghue, M. J., Edwards, E. J., León-
739 Gómez, C., Dawson, T., Camarero Martínez, J. J., Castorena, M., Echeverría, A.,
740 Espinosa, C. I., Fajardo, A., Gazol, A., Isnard, S., Lima, R. S., Marcati, C. R., & Méndez-
741 Alonzo, R. (2018). Plant height and hydraulic vulnerability to drought and cold.
742 *Proceedings of the National Academy of Sciences of the United States of America*,
743 *115*(29), 7551–7556.
744 Parker, T. C., Tang, J., Clark, M. B., Moody, M. M., & Fetcher, N. (2017). Ecotypic differences
745 in the phenology of the tundra species Eriophorum vaginatum reflect sites of origin.
746 *Ecology and Evolution*, *7*(22), 9775–9786.
747 Parker, T. C., Unger, S. L., Moody, M. L., Tang, J., & Fetcher, N. (2021). Intraspecific variation
748 in phenology offers resilience to climate change for Eriophorum vaginatum. *Arctic*
749 *Science*, *AS-2020-0039*, 1–17.
750 Peterson, C. A., Fetcher, N., McGraw, J. B., & Bennington, C. C. (2012). Clinal variation in
751 stomatal characteristics of an Arctic sedge, Eriophorum vaginatum (Cyperaceae).
752 *American Journal of Botany*, *99*(9), 1562–1571.
753 Phoenix, G. K., & Bjerke, J. W. (09/2016). Arctic browning: extreme events and trends reversing
754 arctic greening. *Global Change Biology*, *22*(9), 2960–2962.

Rietze, N., Assmann, J. J., Plekhanova, E., Naegeli, K., Damm, A., Maximov, T., Karsanaev, S. V., Hensgens, G., & Schaepman-Strub, G. (2024). Summer drought weakens land surface cooling of tundra vegetation. *Environmental Research Letters*. https://doi.org/10.1088/1748-9326/ad345e

Sade, N., Del Mar Rubio-Wilhelmi, M., Umnajkitikorn, K., & Blumwald, E. (2018). Stress-induced senescence and plant tolerance to abiotic stress. *Journal of Experimental Botany*, *69*(4), 845–853.

Sáez, P. L., Galmés, J., Ramírez, C. F., Poblete, L., Rivera, B. K., Cavieres, L. A., Clemente-Moreno, M. J., Flexas, J., & Bravo, L. A. (2018). Mesophyll conductance to CO2 is the most significant limitation to photosynthesis at different temperatures and water availabilities in Antarctic vascular species. *Environmental and Experimental Botany*, *156*, 279–287.

Scharn, R., Little, C. J., Bacon, C. D., Alatalo, J. M., Antonelli, A., Björkman, M. P., Molau, U., Nilsson, R. H., & Björk, R. G. (2021). Decreased soil moisture due to warming drives phylogenetic diversity and community transitions in the tundra. *Environmental Research Letters*, *16*(6), 064031.

Schedlbauer, J. L., Fetcher, N., Hood, K., Moody, M. L., & Tang, J. (2018). Effect of growth temperature on photosynthetic capacity and respiration in three ecotypes of Eriophorum vaginatum. *Ecology and Evolution*, *8*(7), 3711–3725.

Shaver, G., Fetcher, N., & Chapin, F. (1986). Growth and Flowering in Eriophorum-Vaginatum - Annual and Latitudinal Variation. *Ecology*, *67*(6), 1524–1535.

Shaver Gaius R., Bret-Harte M. Syndonia, Jones Michael H., Johnstone Jill, Gough Laura, Laundre James, & Chapin F. Stuart. (2001). Species composition interacts with fertilizer to control long-term change in tundra productivity. *Ecology*, *82*(11), 3163–3181.

Souther, S., Fetcher, N., Fowler, Z., Shaver, G. R., & McGraw, J. B. (2014). Ecotypic differentiation in photosynthesis and growth of Eriophorum vaginatum along a latitudinal gradient in the Arctic tundra. *Botany*, *92*(8), 551–561.

Stoner, W. A., & Miller, P. C. (1975). Water relations of plant species in the wet coastal tundra at barrow, Alaska. *Arctic and Alpine Research*, *7*(2), 109–124.

Stunz, E., Fetcher, N., Lavretsky, P., Mohl, J. E., Tang, J., & Moody, M. L. (2022). Landscape genomics provides evidence of ecotypic adaptation and a barrier to gene flow at treeline

for the arctic foundation species Eriophorum vaginatum. *Frontiers in Plant Science*, *13*, 860439.

Sulman, B., Roman, D. T., Yi, K., Wang, L., Phillips, R. P., & Novick, K. (2016). High atmospheric demand for water can limit forest carbon uptake and transpiration as severely as dry soil. *Geophysical Research Letters*, *43*, 9686–9695.

Wein, R. W. (1973). Eriophorum Vaginatum L. *Journal of Ecology*, *61*, 601.

Zona, D., Lafleur, P. M., Hufkens, K., Bailey, B., Gioli, B., Burba, G., Goodrich, J. P., Liljedahl, A. K., Euskirchen, E. S., Watts, J. D., Farina, M., Kimball, J. S., Heimann, M., Göckede, M., Pallandt, M., Christensen, T. R., Mastepanov, M., López-Blanco, E., Jackowicz-Korczynski, M., … Oechel, W. C. (2022). Earlier snowmelt may lead to late season declines in plant productivity and carbon sequestration in Arctic tundra ecosystems. *Scientific Reports*, *12*(1), 3986.

Acknowledgements

Jianwu (Jim) Tang provided valuable mentorship and research leadership through the Ecotypes project, helping to shape both this study and the development of early-career scientists involved in the work. Thomas Parker provided helpful background and methods, including the NDVI-biomass relationship. Thanks to Roger Ruess for loaning the pressure bomb. Thanks to Gus Shaver, Salvatore Curasi, Jeremy May, and Kevin Griffin for insightful suggestions in study design. Special thanks to Robert Michener for lab assistance, and to Steven Unger, Alana Thurston, David Heinz, Matthew Simon, and Sofia Iglesia for field assistance. Pamela Templer provided key research materials and support. This project was supported by the Arctic LTER (NSF-DEB 1026843) and the Toolik Field Station Environmental Data Center. Funding was provided by NSF-OPP #1418010 to N.F., NSF-OPP #1417645 to M.M., and NSF-OPP #1417763 to J.T.

The authors declare no competing interests related to this work.

Author Contributions:

Jon Gewirtzman (JG) and Ned Fetcher (NF) contributed to the study according to the Contributor Roles Taxonomy (CRediT) as follows. Conceptualization was carried out by JG and NF. Data curation, formal analysis, software development, and visualization were performed by JG. Funding acquisition and resource provision were managed by NF. Both JG and NF contributed to investigation, methodology, project administration, and validation. Supervision was provided by NF. Writing of the original draft was led by JG, while both JG and NF participated in reviewing and editing the manuscript. All authors have read and approved the final manuscript.

Data Availability Statement: All code and input data files used for analysis are available at GitHub: https://github.com/jgewirtzman/ecotypes_drying. The full dataset will be published on Dryad upon paper publication and will be accessible via a DOI link at that time.

Supporting Information

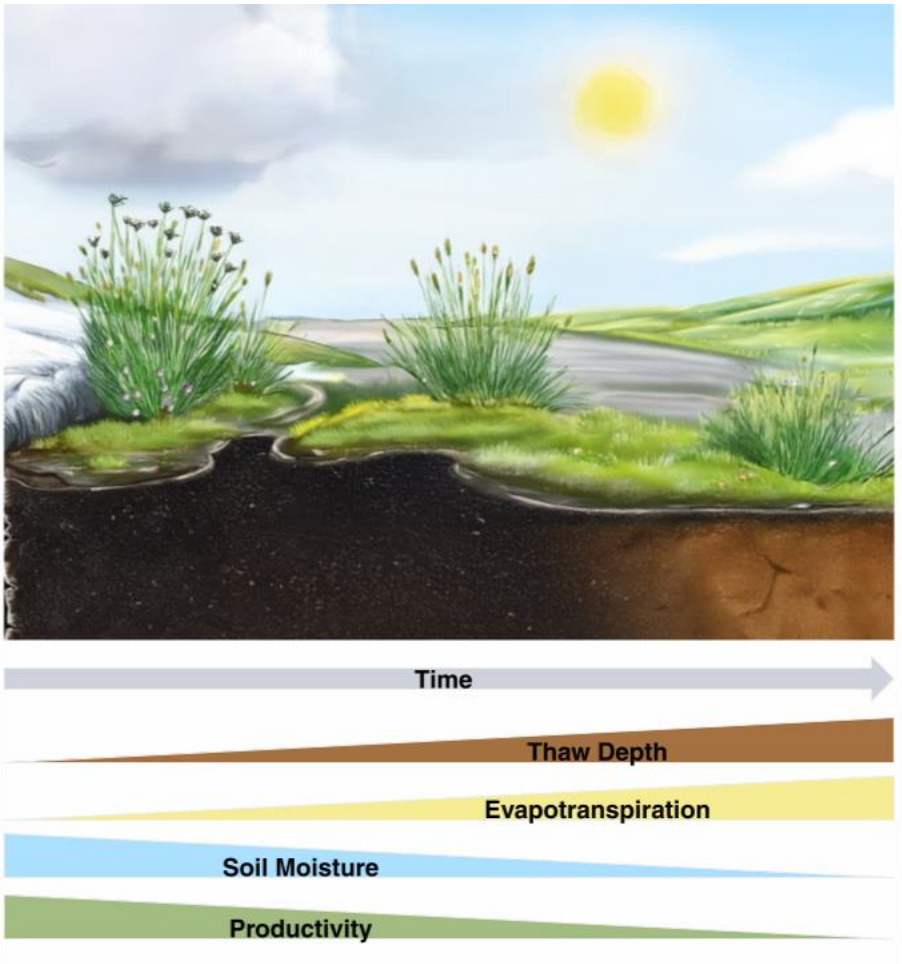

Graphical abstract: Conceptual model of permafrost thaw, soil moisture dynamics, and ecosystem productivity under climate change. The illustration depicts a cross-section of permafrost thaw dynamics, soil moisture variation, and plant growth throughout the growing season. As time progresses, thaw depth increases (brown gradient), leading to enhanced evapotranspiration (yellow gradient). Despite initial high soil moisture (blue gradient), drying occurs due to increased thaw and evapotranspiration. Plant productivity (green gradient) follows a peak-and-decline pattern, reflecting optimal growth conditions early in the season before moisture limitations reduce productivity.

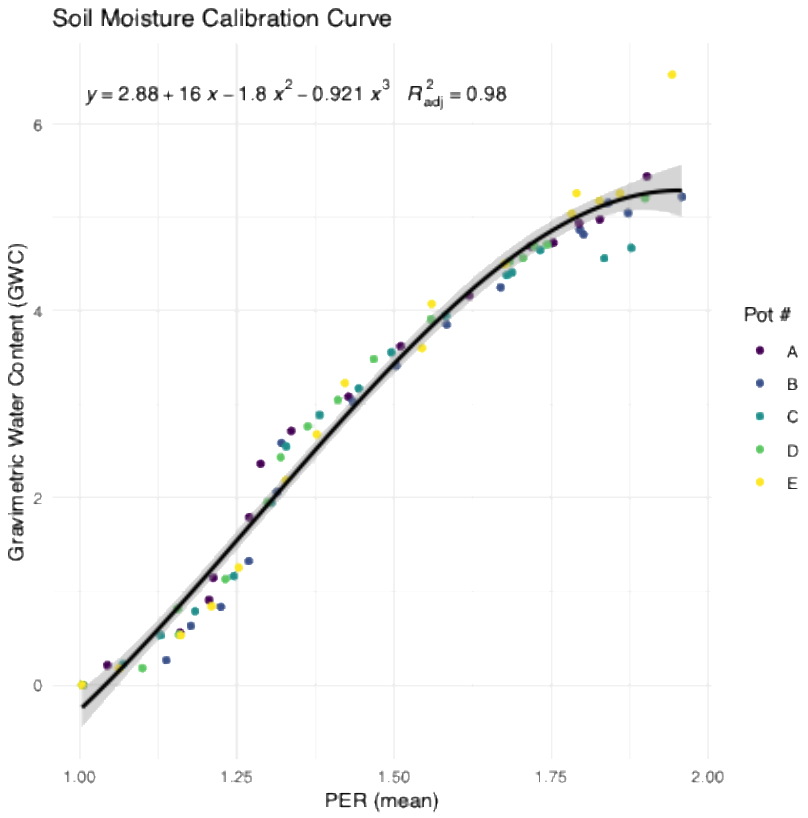

Figure S1. Calibration curve relating relative dielectric permittivity (PER) to gravimetric water content (GWC) for peat soil. Colored points represent measurements from five reference pots during the drying process, and the fitted polynomial regression curve (solid line) includes a shaded 95% confidence interval. This calibration equation ($r^2 = 0.98$) was used to convert HydroSense II probe readings of PER to GWC for field measurements.

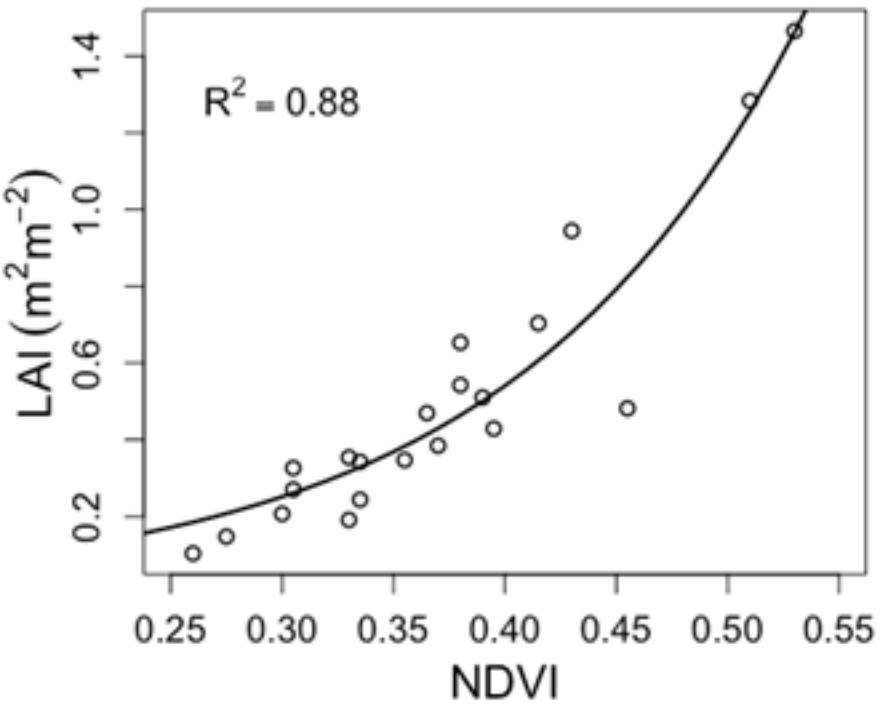

851

852 **Figure S2**. Relationship between Normalized Difference Vegetation Index (NDVI) and Leaf
853 Area Index (LAI) in Arctic tundra vegetation. Each point represents an individual measurement,
854 and the solid line depicts a fitted nonlinear regression model. The relationship is described by the
855 exponential equation:

856 $$LAI = 0.03 \times e^{7.65 \times NDVI}$$

857 with $R^2 = 0.88$, indicating a strong positive correlation between NDVI and LAI.

858

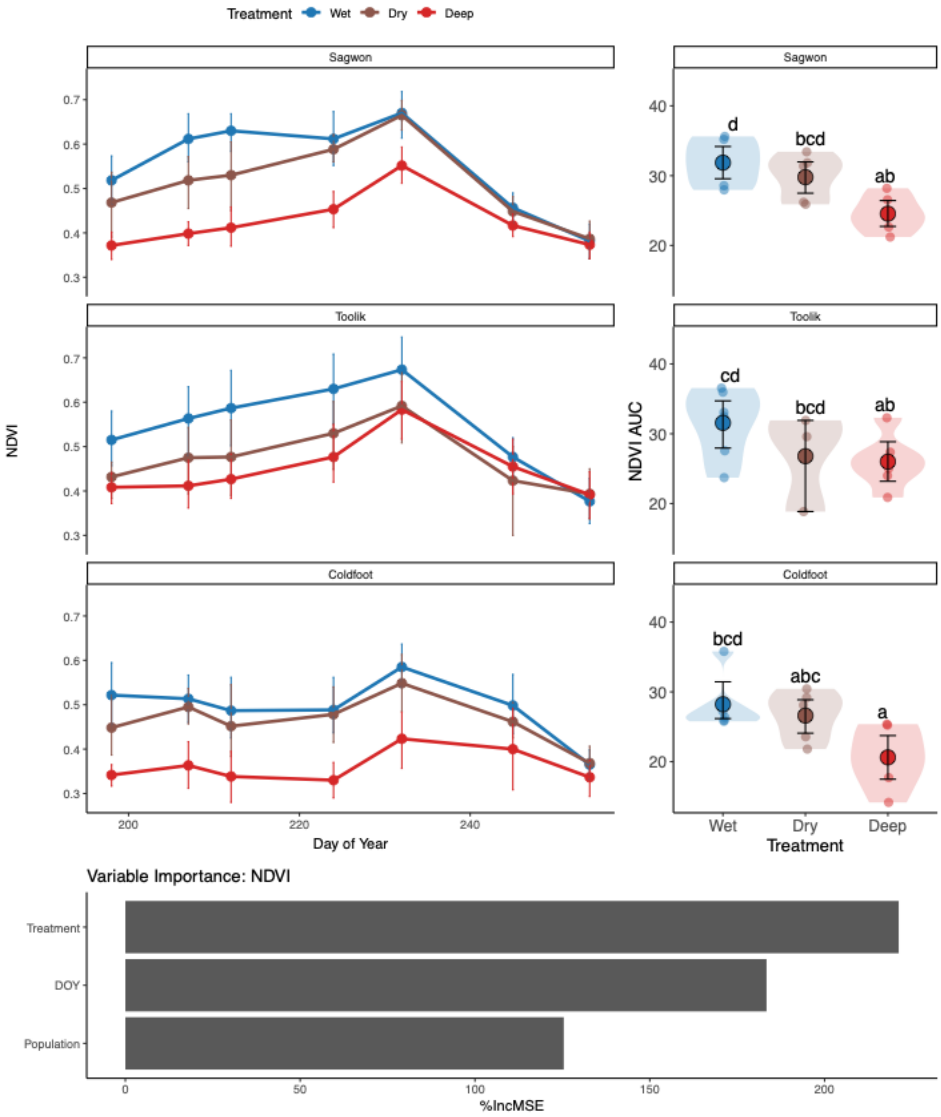

Figure S3. Normalized-difference vegetation index (NDVI) dynamics and cumulative seasonal leaf greenness for E. vaginatum populations (Sagwon, Toolik, and Coldfoot) under three watering treatments in a common garden study. Top left: Time-series plots of NDVI throughout the growing season, with points showing means ± 95% confidence intervals. Top right: Violin plots of area under the curve (AUC) for NDVI, representing total seasonal leaf greenness. Jittered points show individual values, and large circles with error bars indicate estimated marginal means with 95% confidence intervals. Letter annotations above each group indicate significant differences among treatment × population combinations, derived from a quadratic linear mixed-effects model (LME) applied to the longitudinal time-series data ($p < 0.05$). Bottom: Random Forest variable importance plots, with bars ranked by the %IncMSE metric to indicate predictor importance.

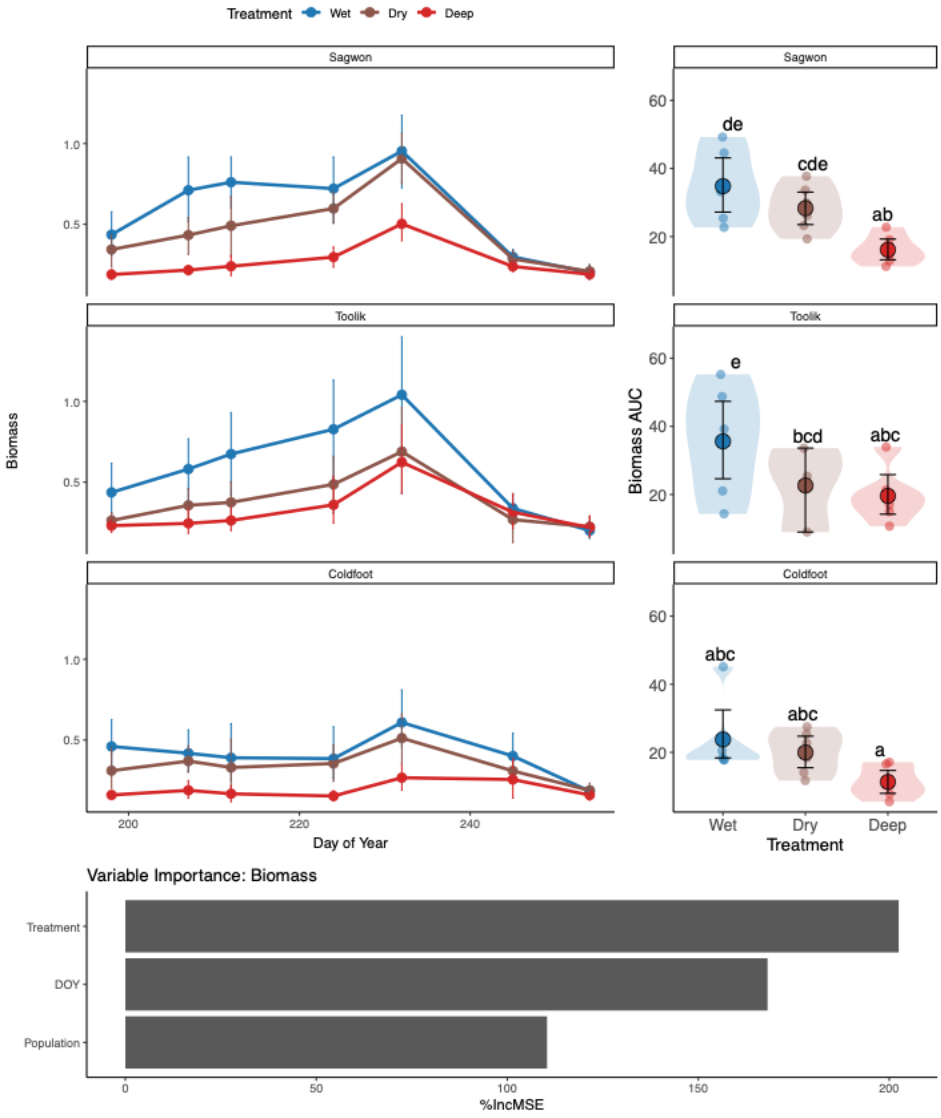

873
874 **Figure S4**. Tussock living biomass dynamics and cumulative seasonal biomass for E. vaginatum
875 populations (Sagwon, Toolik, and Coldfoot) under three watering treatments in a common
876 garden study. Top left: Time-series plots of living biomass throughout the growing season, with
877 points showing means ± 95% confidence intervals. Top right: Violin plots of area under the
878 curve (AUC) for biomass, representing total seasonal time-integrated living biomass. Jittered
879 points show individual values, and large circles with error bars indicate estimated marginal
880 means with 95% confidence intervals. Letter annotations above each group indicate significant
881 differences among treatment × population combinations, derived from a quadratic linear mixed-
882 effects model (LME) applied to the longitudinal time-series data ($p < 0.05$). Bottom: Random
883 Forest variable importance plots, with bars ranked by the %IncMSE metric to indicate predictor
884 importance.
885

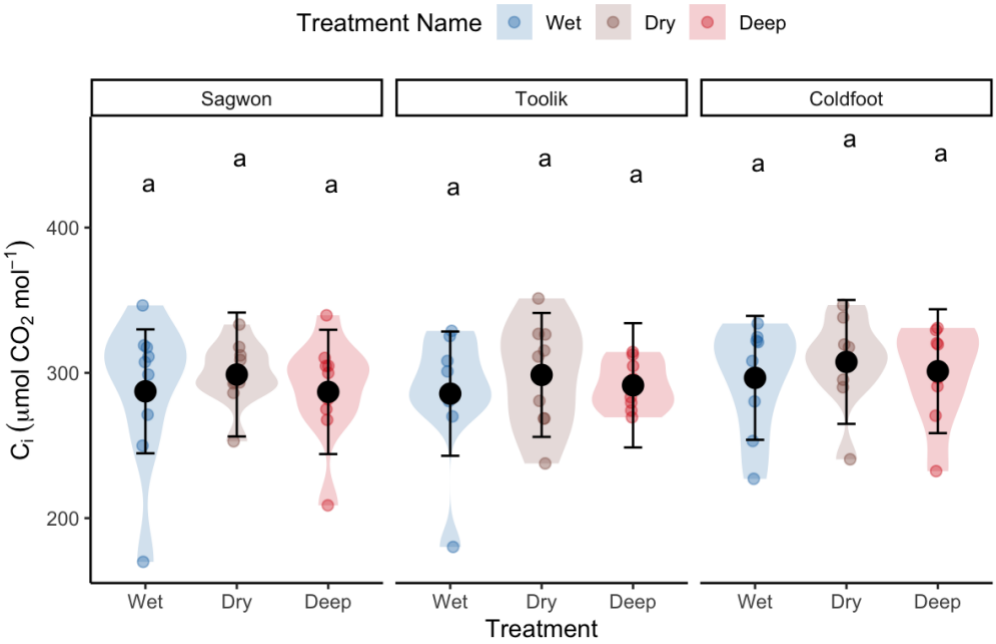

Figure S5. Intercellular CO_2 concentration (C_i, µmol CO_2 mol^{-1}) of *Eriophorum vaginatum* from three populations (Sagwon, Toolik, and Coldfoot) in response to experimental water treatments (Wet, Dry, Deep) in a common garden study. Violin plots display the distribution of raw data, with individual measurements (jittered points), estimated marginal means from mixed-effects models (large filled circles), and their 95% confidence intervals (error bars). Different letters indicate significant differences between treatment × population combinations based on pairwise comparisons with Tukey's adjustment ($p < 0.05$).

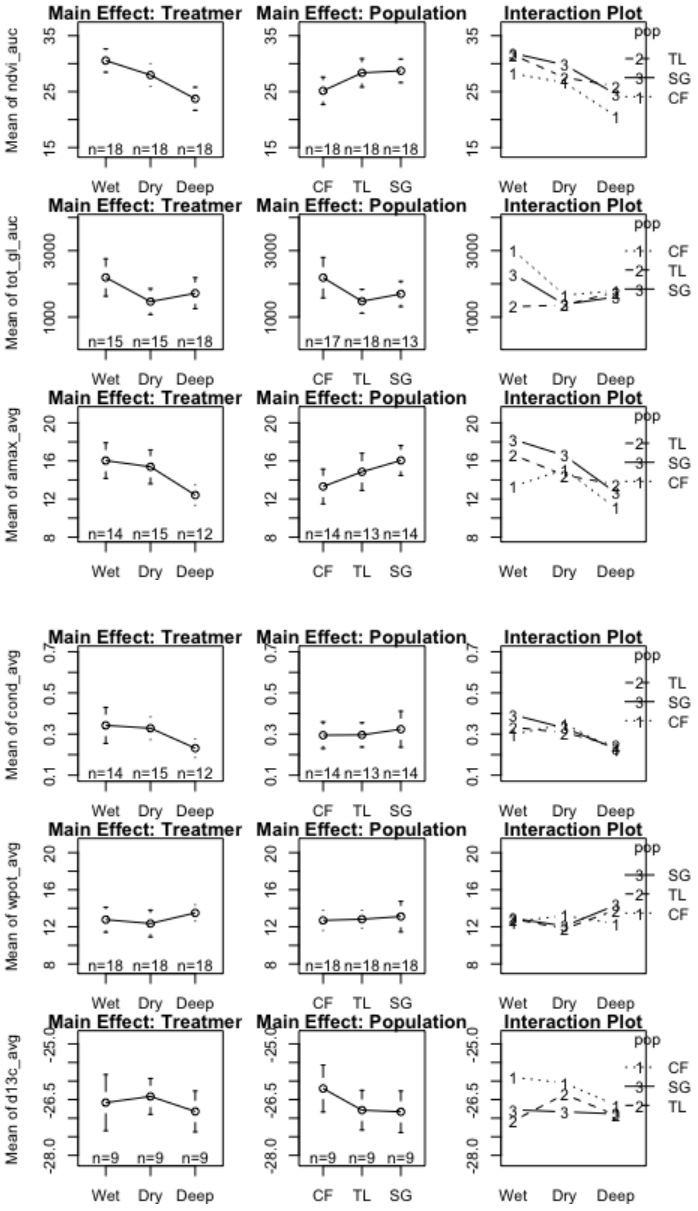

Figure S6. Main effects and interaction effects of water treatment and population on physiological and biochemical traits of *Eriophorum vaginatum*. Each row represents a different trait: (top to bottom) NDVI area under the curve (ndvi_auc), total stomatal conductance area under the curve (tot_g1_auc), maximum photosynthetic rate (amax_avg), stomatal conductance (cond_avg), midday leaf water potential (wpot_avg), and carbon isotope discrimination (d13c_avg).

The left column shows the main effect of water treatment (Wet, Dry, Deep), the middle column shows the main effect of population (CF = Coldfoot, TL = Toolik, SG = Sagwon), and the right column presents interaction plots depicting treatment × population effects. Points represent means ± standard error, and sample sizes (n) are indicated below each group. Interaction plots illustrate how treatment effects vary by population.

Photo S1. Common garden experimental setup at Toolik Field Station. (Top) Potted *Eriophorum vaginatum* tussocks with reflective insulation to minimize soil temperature fluctuations. (Bottom) Transparent tarps supported by rebar and PVC frames covering the Dry and Deep treatment pots to exclude rainfall while maintaining airflow. The experiment simulated three soil moisture regimes: (1) **Wet**, with closed-bottom pots maintained at saturation; (2) **Dry**, with periodic rainfall exclusion; and (3) **Deep**, with extended soil columns allowing deeper drainage and also subjected to rainfall exclusion. Soil moisture, temperature, and photosynthetically active radiation (PAR) were monitored throughout the experiment.

Table S1. Fixed effects summary for phenology models. Estimates, standard errors, degrees of freedom (df), test statistics, and p-values for linear mixed-effects models examining phenological responses of *Eriophorum vaginatum*. The models include responses for (1) Average Green Leaf Length, (2) Tiller Percent Green, and (3) Tiller Total Green Length. Fixed effects include population (Coldfoot, Toolik, Sagwon), water treatment (Wet, Dry, Deep), and their interactions with day of year (DOY) modeled as a second-order polynomial. Significant effects ($p < 0.05$) are indicated in bold. Random effect standard deviations (sd) are reported for intercept and observation-level variation.

Fixed Effects Summary for Phenology Models

Metric	term	estimate	std.error	df	statistic	p.value
Average Green Leaf Length	(Intercept)	6.767	1.021	38.8799	6.625	0
	PopulationColdfoot	1.221	1.445	38.8799	0.845	0.403
	PopulationColdfoot:poly(DOY, 2)1	-14.924	8.493	260.2773	-1.757	0.08
	PopulationColdfoot:poly(DOY, 2)2	15.262	8.531	260.2773	1.789	0.075
	PopulationToolik	-0.504	1.445	38.8799	-0.349	0.729
	PopulationToolik:poly(DOY, 2)1	0.672	8.493	260.2773	0.079	0.937
	PopulationToolik:poly(DOY, 2)2	2.903	8.531	260.2773	0.34	0.734
	`Treatment Name`Dry	-1.136	1.617	39.09142	-0.703	0.487
	`Treatment Name`Dry:PopulationColdfoot	0.592	2.216	38.99235	0.267	0.791
	`Treatment Name`Dry:PopulationColdfoot:poly(DOY, 2)1	1.841	13.021	260.27762	0.141	0.888
	`Treatment Name`Dry:PopulationColdfoot:poly(DOY, 2)2	-11.811	13.185	260.39245	-0.896	0.371
	`Treatment Name`Dry:PopulationToolik	0.907	2.171	39.16585	0.418	0.678
	`Treatment Name`Dry:PopulationToolik:poly(DOY, 2)1	-2.136	12.884	260.38885	-0.166	0.868
	`Treatment Name`Dry:PopulationToolik:poly(DOY, 2)2	1.903	12.906	260.39786	0.147	0.883
	`Treatment Name`Dry:poly(DOY, 2)1	-3.934	9.496	260.27789	-0.414	0.679
	`Treatment Name`Dry:poly(DOY, 2)2	2.288	9.684	260.49068	0.236	0.813
	`Treatment Name`Wet	2.239	1.769	38.8799	1.265	0.213
	`Treatment Name`Wet:PopulationColdfoot	2.794	2.284	38.8799	1.223	0.229
	`Treatment Name`Wet:PopulationColdfoot:poly(DOY, 2)1	17.342	13.429	260.2773	1.291	0.198
	`Treatment Name`Wet:PopulationColdfoot:poly(DOY, 2)2	-38.058	13.489	260.2773	-2.821	0.005
	`Treatment Name`Wet:PopulationToolik	-1.773	2.292	39.35969	-0.774	0.444
	`Treatment Name`Wet:PopulationToolik:poly(DOY, 2)1	16.002	13.899	262.38736	1.151	0.251
	`Treatment Name`Wet:PopulationToolik:poly(DOY, 2)2	-7.141	13.748	260.48163	-0.519	0.604
	`Treatment Name`Wet:poly(DOY, 2)1	-26.827	10.402	260.2773	-2.579	0.01
	`Treatment Name`Wet:poly(DOY, 2)2	-8.164	10.449	260.2773	-0.781	0.435
	poly(DOY, 2)1	-29.579	6.006	260.2773	-4.925	0

	poly(DOY, 2)2	-12.657	6.032	260.2773	-2.098	0.037
	sd__(Intercept)	2.366	NA	NA	NA	NA
	sd__Observation	2.156	NA	NA	NA	NA
Tiller Percent Green	(Intercept)	0.778	0.078	38.87542	9.944	0
	PopulationColdfoot	-0.237	0.111	38.87542	-2.143	0.038
	PopulationColdfoot:poly(DOY, 2)1	-0.024	0.549	260.16349	-0.044	0.965
	PopulationColdfoot:poly(DOY, 2)2	1.672	0.552	260.16349	3.032	0.003
	PopulationToolik	-0.056	0.111	38.87542	-0.508	0.614
	PopulationToolik:poly(DOY, 2)1	-0.454	0.549	260.16349	-0.826	0.409
	PopulationToolik:poly(DOY, 2)2	0.173	0.552	260.16349	0.313	0.755
	`Treatment Name`Dry	-0.2	0.124	39.02747	-1.615	0.114
	`Treatment Name`Dry:PopulationColdfoot	0.222	0.17	38.95627	1.309	0.198
	`Treatment Name`Dry:PopulationColdfoot:poly(DOY, 2)1	-0.208	0.842	260.16372	-0.247	0.805
	`Treatment Name`Dry:PopulationColdfoot:poly(DOY, 2)2	-1.536	0.852	260.24637	-1.802	0.073
	`Treatment Name`Dry:PopulationToolik	0.126	0.166	39.08066	0.76	0.452
	`Treatment Name`Dry:PopulationToolik:poly(DOY, 2)1	0.578	0.833	260.24359	0.694	0.488
	`Treatment Name`Dry:PopulationToolik:poly(DOY, 2)2	-0.507	0.834	260.25026	-0.608	0.544
	`Treatment Name`Dry:poly(DOY, 2)1	-0.235	0.614	260.16392	-0.383	0.702
	`Treatment Name`Dry:poly(DOY, 2)2	0.699	0.626	260.31708	1.116	0.265
	`Treatment Name`Wet	-0.089	0.135	38.87542	-0.659	0.514
	`Treatment Name`Wet:PopulationColdfoot	0.342	0.175	38.87542	1.954	0.058
	`Treatment Name`Wet:PopulationColdfoot:poly(DOY, 2)1	0.62	0.868	260.16349	0.714	0.476
	`Treatment Name`Wet:PopulationColdfoot:poly(DOY, 2)2	-1.985	0.872	260.16349	-2.276	0.024
	`Treatment Name`Wet:PopulationToolik	0.057	0.175	39.23111	0.324	0.748
	`Treatment Name`Wet:PopulationToolik:poly(DOY, 2)1	0.385	0.899	261.7314	0.428	0.669
	`Treatment Name`Wet:PopulationToolik:poly(DOY, 2)2	-0.422	0.889	260.31519	-0.474	0.636
	`Treatment Name`Wet:poly(DOY, 2)1	-1.081	0.672	260.16349	-1.607	0.109
	`Treatment Name`Wet:poly(DOY, 2)2	-0.511	0.675	260.16349	-0.757	0.45
	poly(DOY, 2)1	-2.9	0.388	260.16349	-7.468	0
	poly(DOY, 2)2	-1.658	0.39	260.16349	-4.251	0
	sd__(Intercept)	0.184	NA	NA	NA	NA
	sd__Observation	0.139	NA	NA	NA	NA
Tiller Total Green Length	(Intercept)	26.407	5.381	38.9615	4.908	0
	PopulationColdfoot	3.528	7.61	38.9615	0.464	0.646
	PopulationColdfoot:poly(DOY, 2)1	-14.688	31.258	260.16107	-0.47	0.639
	PopulationColdfoot:poly(DOY, 2)2	22.847	31.397	260.16107	0.728	0.467

	PopulationToolik	2.086	7.61	38.9615	0.274	0.785
	PopulationToolik:poly(DOY, 2)1	1.456	31.258	260.16107	0.047	0.963
	PopulationToolik:poly(DOY, 2)2	-34.136	31.397	260.16107	-1.087	0.278
	`Treatment Name`Dry	-3.223	8.514	39.06639	-0.379	0.707
	`Treatment Name`Dry:PopulationColdfoot	0.491	11.67	39.01728	0.042	0.967
	`Treatment Name`Dry:PopulationColdfoot:poly(DOY, 2)1	21.01	47.919	260.16123	0.438	0.661
	`Treatment Name`Dry:PopulationColdfoot:poly(DOY, 2)2	-14.896	48.526	260.21809	-0.307	0.759
	`Treatment Name`Dry:PopulationToolik	-2.229	11.425	39.10292	-0.195	0.846
	`Treatment Name`Dry:PopulationToolik:poly(DOY, 2)1	57.806	47.42	260.21607	1.219	0.224
	`Treatment Name`Dry:PopulationToolik:poly(DOY, 2)2	28.7	47.502	260.22076	0.604	0.546
	`Treatment Name`Dry:poly(DOY, 2)1	-75.8	34.949	260.16137	-2.169	0.031
	`Treatment Name`Dry:poly(DOY, 2)2	11.117	35.643	260.26673	0.312	0.755
	`Treatment Name`Wet	11.949	9.32	38.9615	1.282	0.207
	`Treatment Name`Wet:PopulationColdfoot	6.771	12.032	38.9615	0.563	0.577
	`Treatment Name`Wet:PopulationColdfoot:poly(DOY, 2)1	60.483	49.424	260.16107	1.224	0.222
	`Treatment Name`Wet:PopulationColdfoot:poly(DOY, 2)2	-81.909	49.643	260.16107	-1.65	0.1
	`Treatment Name`Wet:PopulationToolik	-14.55	12.052	39.213	-1.207	0.235
	`Treatment Name`Wet:PopulationToolik:poly(DOY, 2)1	68.444	51.209	261.26754	1.337	0.183
	`Treatment Name`Wet:PopulationToolik:poly(DOY, 2)2	66.075	50.6	260.26806	1.306	0.193
	`Treatment Name`Wet:poly(DOY, 2)1	-120.314	38.283	260.16107	-3.143	0.002
	`Treatment Name`Wet:poly(DOY, 2)2	-71.129	38.454	260.16107	-1.85	0.065
	poly(DOY, 2)1	-58.327	22.103	260.16107	-2.639	0.009
	poly(DOY, 2)2	-81.488	22.201	260.16107	-3.67	0
	sd__(Intercept)	12.835	NA	NA	NA	NA
	sd__Observation	7.935	NA	NA	NA	NA

932
933

Table S2. Fixed effects summary for canopy models. Estimates, standard errors, degrees of freedom (df), test statistics, and p-values for linear mixed-effects models examining canopy responses of *Eriophorum vaginatum*. The models include responses for (1) Biomass, (2) LAI, and (3) NDVI. Fixed effects include population (Coldfoot, Toolik, Sagwon), water treatment (Wet, Dry, Deep), and their interactions with day of year (DOY) modeled as a second-order polynomial. Significant effects ($p < 0.05$) are indicated in bold. Random effect standard deviations (sd) are reported for intercept and observation-level variation.

Fixed Effects Summary for Canopy Models

Metric	term	estimate	std.error	df	statistic	p.value
Biomass	(Intercept)	0.583	0.062	44.86963	9.399	0
	PopulationColdfoot	-0.176	0.088	44.86963	-2.009	0.051
	PopulationToolik	0.003	0.088	44.86963	0.03	0.976
	TreatmentDeep	-0.315	0.088	44.86963	-3.595	0.001
	TreatmentDeep:PopulationColdfoot	0.102	0.124	44.86963	0.819	0.417
	TreatmentDeep:PopulationToolik	0.052	0.124	44.86963	0.419	0.677
	TreatmentDry	-0.116	0.088	44.86963	-1.328	0.191
	TreatmentDry:PopulationColdfoot	0.049	0.124	44.86963	0.394	0.695
	TreatmentDry:PopulationToolik	-0.079	0.124	45.17777	-0.633	0.53
	poly(DOY, 2)1	-2.19	0.471	302.9967	-4.645	0
	poly(DOY, 2)1:PopulationColdfoot	1.221	0.667	302.9967	1.832	0.068
	poly(DOY, 2)1:PopulationToolik	0.692	0.667	302.9967	1.039	0.3
	poly(DOY, 2)1:TreatmentDeep	2.512	0.667	302.9967	3.769	0
	poly(DOY, 2)1:TreatmentDeep:PopulationColdfoot	-1.229	0.943	302.9967	-1.304	0.193
	poly(DOY, 2)1:TreatmentDeep:PopulationToolik	-0.491	0.943	302.9967	-0.521	0.603
	poly(DOY, 2)1:TreatmentDry	1.521	0.667	302.9967	2.282	0.023
	poly(DOY, 2)1:TreatmentDry:PopulationColdfoot	-1.057	0.943	302.9967	-1.122	0.263
	poly(DOY, 2)1:TreatmentDry:PopulationToolik	0.034	0.955	303.2141	0.036	0.971
	poly(DOY, 2)2	-3.889	0.471	302.9967	-8.25	0
	poly(DOY, 2)2:PopulationColdfoot	2.725	0.667	302.9967	4.088	0
	poly(DOY, 2)2:PopulationToolik	-0.511	0.667	302.9967	-0.767	0.444
	poly(DOY, 2)2:TreatmentDeep	2.495	0.667	302.9967	3.742	0
	poly(DOY, 2)2:TreatmentDeep:PopulationColdfoot	-1.656	0.943	302.9967	-1.757	0.08
	poly(DOY, 2)2:TreatmentDeep:PopulationToolik	0.175	0.943	302.9967	0.185	0.853
	poly(DOY, 2)2:TreatmentDry	0.589	0.667	302.9967	0.883	0.378
	poly(DOY, 2)2:TreatmentDry:PopulationColdfoot	-0.686	0.943	302.9967	-0.727	0.468
	poly(DOY, 2)2:TreatmentDry:PopulationToolik	1.441	0.943	302.99686	1.529	0.127
	sd__(Intercept)	0.14	NA	NA	NA	NA
	sd__Observation	0.157	NA	NA	NA	NA
LAI	(Intercept)	2.951	0.405	44.86326	7.285	0

	PopulationColdfoot	-1.207	0.573	44.86326	-2.108	0.041
	PopulationToolik	0.117	0.573	44.86326	0.204	0.84
	TreatmentDeep	-2.019	0.573	44.86326	-3.524	0.001
	TreatmentDeep:PopulationColdfoot	0.859	0.81	44.86326	1.061	0.294
	TreatmentDeep:PopulationToolik	0.213	0.81	44.86326	0.263	0.793
	TreatmentDry	-0.815	0.573	44.86326	-1.423	0.162
	TreatmentDry:PopulationColdfoot	0.395	0.81	44.86326	0.488	0.628
	TreatmentDry:PopulationToolik	-0.572	0.812	45.23361	-0.705	0.484
	poly(DOY, 2)1	-12.772	3.385	303.01618	-3.773	0
	poly(DOY, 2)1:PopulationColdfoot	7.618	4.787	303.01618	1.591	0.113
	poly(DOY, 2)1:PopulationToolik	4.621	4.787	303.01618	0.965	0.335
	poly(DOY, 2)1:TreatmentDeep	14.502	4.787	303.01618	3.03	0.003
	poly(DOY, 2)1:TreatmentDeep:PopulationColdfoot	-7.756	6.769	303.01618	-1.146	0.253
	poly(DOY, 2)1:TreatmentDeep:PopulationToolik	-3.143	6.769	303.01618	-0.464	0.643
	poly(DOY, 2)1:TreatmentDry	9.832	4.787	303.01618	2.054	0.041
	poly(DOY, 2)1:TreatmentDry:PopulationColdfoot	-7.278	6.769	303.01618	-1.075	0.283
	poly(DOY, 2)1:TreatmentDry:PopulationToolik	-0.478	6.858	303.27741	-0.07	0.944
	poly(DOY, 2)2	-25.886	3.385	303.01618	-7.648	0
	poly(DOY, 2)2:PopulationColdfoot	19.183	4.787	303.01618	4.007	0
	poly(DOY, 2)2:PopulationToolik	-5.325	4.787	303.01618	-1.113	0.267
	poly(DOY, 2)2:TreatmentDeep	18.688	4.787	303.01618	3.904	0
	poly(DOY, 2)2:TreatmentDeep:PopulationColdfoot	-13.517	6.769	303.01618	-1.997	0.047
	poly(DOY, 2)2:TreatmentDeep:PopulationToolik	2.34	6.769	303.01618	0.346	0.73
	poly(DOY, 2)2:TreatmentDry	5.151	4.787	303.01618	1.076	0.283
	poly(DOY, 2)2:TreatmentDry:PopulationColdfoot	-5.325	6.769	303.01618	-0.787	0.432
	poly(DOY, 2)2:TreatmentDry:PopulationToolik	11.359	6.77	303.01637	1.678	0.094
	sd__(Intercept)	0.896	NA	NA	NA	NA
	sd__Observation	1.128	NA	NA	NA	NA
NDVI	(Intercept)	0.554	0.028	44.90651	19.925	0
	PopulationColdfoot	-0.06	0.039	44.90651	-1.531	0.133
	PopulationToolik	-0.008	0.039	44.90651	-0.212	0.833
	TreatmentDeep	-0.129	0.039	44.90651	-3.28	0.002
	TreatmentDeep:PopulationColdfoot	-0.003	0.056	44.90651	-0.056	0.956
	TreatmentDeep:PopulationToolik	0.034	0.056	44.90651	0.603	0.549
	TreatmentDry	-0.039	0.039	44.90651	-0.999	0.323
	TreatmentDry:PopulationColdfoot	0.01	0.056	44.90651	0.175	0.862
	TreatmentDry:PopulationToolik	-0.028	0.056	45.10944	-0.497	0.622
	poly(DOY, 2)1	-1.063	0.171	302.99002	-6.229	0
	poly(DOY, 2)1:PopulationColdfoot	0.475	0.241	302.99002	1.968	0.05

	poly(DOY, 2)1:PopulationToolik	0.258	0.241	302.99002	1.068	0.286
	poly(DOY, 2)1:TreatmentDeep	1.252	0.241	302.99002	5.186	0
	poly(DOY, 2)1:TreatmentDeep:PopulationColdfoot	-0.471	0.341	302.99002	-1.378	0.169
	poly(DOY, 2)1:TreatmentDeep:PopulationToolik	-0.236	0.341	302.99002	-0.692	0.49
	poly(DOY, 2)1:TreatmentDry	0.613	0.241	302.99002	2.538	0.012
	poly(DOY, 2)1:TreatmentDry:PopulationColdfoot	-0.35	0.341	302.99002	-1.025	0.306
	poly(DOY, 2)1:TreatmentDry:PopulationToolik	0.068	0.346	303.13312	0.196	0.845
	poly(DOY, 2)2	-1.456	0.171	302.99002	-8.528	0
	poly(DOY, 2)2:PopulationColdfoot	0.825	0.241	302.99002	3.417	0.001
	poly(DOY, 2)2:PopulationToolik	-0.045	0.241	302.99002	-0.184	0.854
	poly(DOY, 2)2:TreatmentDeep	0.577	0.241	302.99002	2.388	0.018
	poly(DOY, 2)2:TreatmentDeep:PopulationColdfoot	-0.174	0.341	302.99002	-0.511	0.61
	poly(DOY, 2)2:TreatmentDeep:PopulationToolik	0.064	0.341	302.99002	0.189	0.85
	poly(DOY, 2)2:TreatmentDry	0.052	0.241	302.99002	0.217	0.829
	poly(DOY, 2)2:TreatmentDry:PopulationColdfoot	-0.138	0.341	302.99002	-0.404	0.687
	poly(DOY, 2)2:TreatmentDry:PopulationToolik	0.417	0.341	302.99013	1.22	0.223
	sd__(Intercept)	0.065	NA	NA	NA	NA
	sd__Observation	0.057	NA	NA	NA	NA